AD-A107 759 AVCO EVERETT RESEARCH LAB INC EVERETT MA F/G 20/5
RECYCLABILITY ISSUES IN XEF LASERS.(U)
AUG 81 A MANDL, R SLATER, D TRAINOR F33615-80-C-2060
UNCLASSIFIED AFWAL-TR-81-2085 NL

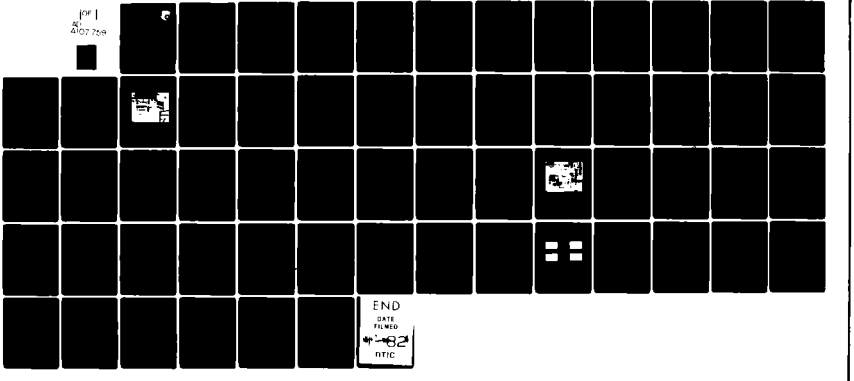

AFWAL-TR-81-2085

RECYCLABILITY ISSUES IN XeF LASERS

A. MANDL, R. SLATER AND D. TRAINOR

AVCO EVERETT RESEARCH LABORATORY, INC.
A SUBSIDIARY OF AVCO CORPORATION
2385 REVERE BEACH PARKWAY
EVERETT, MA 02149

AUGUST 1981

FINAL TECHNICAL REPORT FOR PERIOD 15 JUNE 1980 – 15 APRIL 1981

Approved for public release; distribution unlimited.

PROPULSION LABORATORY
AIR FORCE WRIGHT AERONAUTICAL LABORATORIES
AIR FORCE SYSTEMS COMMAND
WRIGHT-PATTERSON AIR FORCE BASE, OHIO 45433

NOTICE

When Government drawings, specifications, or other data are used for any purpose other than in connection with a definitely related Government procurement operation, the United States Government thereby incurs no responsibility nor any obligation whatsoever; and the fact that the government may have formulated, furnished, or in any way supplied the said drawings, specifications, or other data, is not to be regarded by implication or otherwise as in any manner licensing the holder or any other person or corporation, or conveying any rights or permission to manufacture use, or sell any patented invention that may in any way be related thereto.

This report has been reviewed by the Office of Public Affairs (ASD/PA) and is releasable to the National Technical Information Service (NTIS). At NTIS, it will be available to the general public, including foreign nations.

This technical report has been reviewed and is approved for publication.

PROJECT ENGINEER
AFWAL/POOC-3

ROBERT R. BARTHELEMY
Chief, Energy Conversion Branch
Aerospace Power Division
Aero Propulsion Laboratory

FOR THE COMMANDER

JAMES D. REAMS
Chief, Aerospace Power Division
Aero Propulsion Laboratory

"If your address has changed, if you wish to be removed from our mailing list, or if the addressee is no longer employed by your organization please notify AFWAL/POOC, *W-PAFB, OH 45433 to help us maintain a current mailing list".*

Copies of this report should not be returned unless return is required by security considerations, contractual obligations, or notice on a specific document.

AIR FORCE/56780/19 November 1981 — 170

UNCLASSIFIED

SECURITY CLASSIFICATION OF THIS PAGE *(When Data Entered)*

REPORT DOCUMENTATION PAGE	READ INSTRUCTIONS BEFORE COMPLETING FORM
1 REPORT NUMBER: AFWAL-TR-81-2085	2 GOVT ACCESSION NO: AD-A107759
3 RECIPIENT'S CATALOG NUMBER	
4 TITLE *(and Subtitle)*: RECYCLABILITY ISSUES IN XeF LASERS	5 TYPE OF REPORT & PERIOD COVERED: Final Technical Report 15 June 1980-15 April 1981
	6 PERFORMING ORG. REPORT NUMBER
7 AUTHOR(s): A. Mandl, R. Slater and D. Trainor	8 CONTRACT OR GRANT NUMBER(s): F33615-80-C-2060
9 PERFORMING ORGANIZATION NAME AND ADDRESS: Avco Everett Research Laboratory, Inc. 2385 Revere Beach Parkway Everett, MA 02149	10 PROGRAM ELEMENT PROJECT TASK AREA & WORK UNIT NUMBERS: 62301E 3938
11 CONTROLLING OFFICE NAME AND ADDRESS: Propulsion Laboratory (AFWAL/POOC) AF Wright Aeronautical Laboratories AFSC Wright-Patterson AF Base, Ohio 45433	12 REPORT DATE: August 1981
	13 NUMBER OF PAGES: 52
14 MONITORING AGENCY NAME & ADDRESS *(if different from Controlling Office)*	15 SECURITY CLASS. *(of this report)*: UNCLASSIFIED
	15a DECLASSIFICATION DOWNGRADING SCHEDULE

16 DISTRIBUTION STATEMENT *(of this Report)*

Approved for public release; distribution unlimited

17 DISTRIBUTION STATEMENT *(of the abstract entered in Block 20, if different from Report)*

18 SUPPLEMENTARY NOTES

19 KEY WORDS *(Continue on reverse side if necessary and identify by block number)*

XeF Laser
Recyclability
Materials Compatibility
F_2 Scrubbers,
NF_3
NF_2
F_2

20 ABSTRACT *(Continue on reverse side if necessary and identify by block number)*

This report describes three experiments designed to assess various aspects of XeF laser operation at elevated temperatures. Measurements of the rate of loss of NF_3 and NF_2 in contact with metals and quartz were obtained in one experiment. Nickel, quartz and aluminum appear to be less reactive than titanium, stainless steel and copper.

DD FORM 1 JAN 73 1473 EDITION OF 1 NOV 65 IS OBSOLETE

UNCLASSIFIED

SECURITY CLASSIFICATION OF THIS PAGE *(When Data Entered)*

The feasibility of using metal-filled reactors to scrub F_2 from XeF laser gas mixtures was investigated. Titanium was shown to be a selective F_2 scrubber.

XeF laser performance was studied as a function of NF_3 and NF_2 mole fractions. These experiments indicate that the presence of NF_2 degrades laser performance using a stainless steel cell. The cell construction material appears to play a significant role in determining the extent of degradation.

FOREWORD

This technical report was accomplished under Project 2301, Work Unit 2301S283 "Recyclability Issues in XeF Lasers". The study was performed by the Avco Everett Research Laboratory, Inc. under contract F33615-80-C-2060 and funded by the Directed Energy Office, Defense Advanced Research Projects Agency. The DARPA program manager was Lt Col R. P. Benedict, Jr., and the Air Force program manager was Dr Alan Garscadden, Energy Conversion Branch, Aero Propulsion Laboratory, Wright-Patterson AFB.

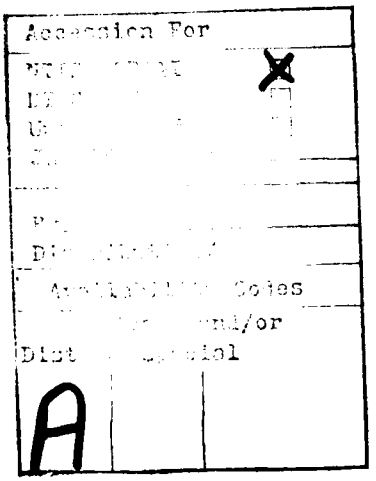

TABLE OF CONTENTS

LIST OF ILLUSTRATIONS

I. INTRODUCTION

High energy, efficient operation of xenon fluoride lasers has been demonstrated by a number of groups.[1,2,3] Subsequently, output energy, laser intrinsic efficiency and specific energy (J/ℓ-AMG) have been shown[4] to increase when the laser is operated at elevated temperature ($\sim 450^{o}K$). Current DARPA programs[5] are investigating the feasibility and limitation in scaling xenon fluoride to high single pulse output at $300^{o}K$ as well as elevated temperatures. Future efforts will be directed to demonstrate that this laser system can be operated in a repetitively-pulsed mode to produce high average power and eventually with closed-cycle operation without significant degradation of the laser performance for extended periods of operation.

At room temperature, the laser mixture shows evidence for little degradation over extended periods of time when repeatedly irradiated with a high energy e-beam (see Figure 1). This suggests that at this temperature, in this laser cavity (stainless steel, aluminized kapton, quartz, o-rings, etc.), the laser gas components are compatible with the cavity materials and the gas phase homogeneous chemistry is favorable for relasing the same

(1) Hsia, J.C., Jacob, J.H., Mangano, J.A., Rokni, M., Semi-Annual Report 1-Meter Laser System, 23 February 1977 - 22 August 1977.

(2) Hunter, R.O., Jr. Private communication.

(3) Champagne, L.F., Harris, N.W., App. Phys. Lett 31, 513 (1977).

(4) Hsia, J.C., Mangano, J.A., Jacob, J.H., and Rokni, M., App. Phys. Lett 34, 208 (1979).

(5) Visible Laser Scale-Up (Contract DAAK40-79-C-0197).

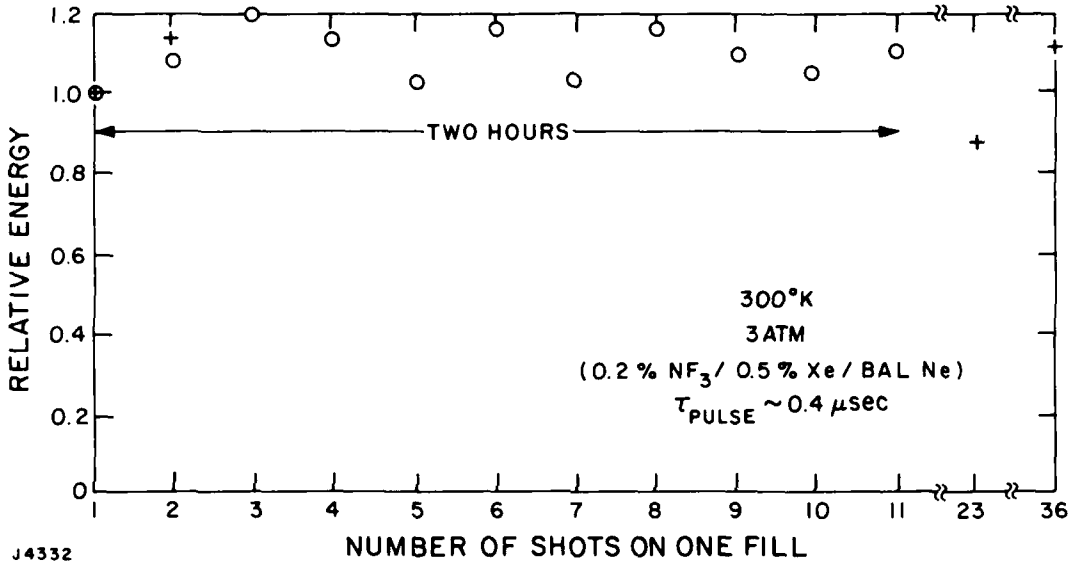

Figure 1 Relative Laser Output Energy vs The Number of Repeated E-Beam Irradiations on a Single Fill(1-M Device)

fuel. This suggests that the rate constants which define the rate of change in the fluorine atom density with time favors the reformation of NF_3, i.e.,

$$F + NF_2 + M \rightarrow NF_3 + M \quad (1)$$

dominates and/or the production of F_2 by the reaction

$$F + F + M \rightarrow F_2 + M \quad (2)$$

does not cause any loss in laser performance. It is well established that F_2 is an efficient donor for the production of XeF* in the upper laser state[6] but has significant absorption at the laser operating wavelength of 350 nm.[7]

At 300°K, the rate for reaction (1) is 100X to 1000X faster than the rate for reaction (2). This estimate was obtained using the rate constants available from the literature[8,9] and the pressure scaling suggested by Smith and Heustis[10] for reaction (1) and applying these to our experimental conditions of pressure and mixture mole fractions.

At elevated temperatures, consideration of the calculated[10] negative temperature dependence of reaction (1) relative to an assumed temperature independent behavior for reaction (2), these rates may only differ by 10X to 100X in favor

(6) Rokni, M., Jacob, J.H., Mangano, J.A. and Brochu, R., App. Phys. Lett. 32, 223 (1978).

(7) Calvert, J.G. and Pitts, J.N., Jr., Photochemistry (Wiley, New York, 1966).

(8) Tang, K.Y., Hunter, R.O., Jr. and Heustis, D.L., (submitted to J. App. Phys., 1981).

(9) Lloyd, A.C., Int. J. Chem. Kin 3, 39 (1971).

(10) Smith, G.P. and Heustis, D.L., (submitted to J. App. Phys., 1981).

of reformation of the NF_3 fuel. Clearly, laser degradation at elevated temperature is a more serious concern. Regardless of these rates and their ratios, however, there will be some buildup of F_2, and perhaps other fluoride compounds, as a result of homogeneous and heterogeneous chemical reactions.

To investigate these effects, we carried out the program described in this final report. Our program consisted of three tasks. The first entitled "gas scrubbing" was undertaken to explore techniques to remove the F_2 from mixtures of F_2, NF_3, Xe and Ne. The second task provided information on the compatibility of NF_3 and NF_2 radicals with likely laser construction materials. The third investigated the impact of NF_2 radicals on laser performance.

The results of these tasks are described in detail in the following sections.

II. F_2 SCRUBBING

A. INTRODUCTION

The rare-gas halide excimer lasers are the most efficient sources of laser radiation at visible and ultraviolet wavelengths. Of particular interest to DARPA is the xenon fluoride laser which can propagate through the atmosphere due to its lasing wavelength of ~ 351 nm.

A typical XeF laser mixture consists of 0.2% NF_3/0.5% Xe/99.3% Ne. Since these rare gases are quite costly, it is necessary for a cost efficient system that the rare gases be recovered and reused, i.e., recycled. A problem, however, is that during reactions that result in the formation of the upper laser level, NF_3 dissociates to form NF_2 radicals and F^- ions. After lasing, the XeF lower laser level dissociates and some fraction of the resultant free fluorine atoms will recombine to form F_2 which absorbs at the laser wavelength and, therefore, for any large-scale closed-cycle system must be removed. Recycling the laser mixture, therefore, at a minimum involves separating the F_2 contaminant from the mixture of $F_2/NF_3/Xe/Ne$.

There are several possible approaches to removing F_2 from the laser mixture; selective distillation, catalytic reaction with Xe, wet (or dry) scrubbing, etc. Since F_2 liquifies at 50^oK, distillation is very energy inefficient requiring that the entire mixture be cooled and then reheated after separation. An alternate possibility is to react F_2 with Xe either catalytically or by using a discharge to form XeF_n (n = 2,4,6). Since the xenon fluorides have significantly lower vapor pressures than fluorine (<1 torr at $T = 0^oC$), one could distill the xenon fluoride compounds more economically than molecular fluorine. Alternately, one could use heterogeneous chemistry to selectively react the

fluorine on a surface. Here again there are several approaches possible. There are the wet chemical methods using NaOH or KOH caustic scrubbers to form alkali fluoride salts. These require cold traps to remove deleterious water vapor from the system. There is also the dry chemistry approach using metal scrubbers. This approach takes advantage of the tendency of fluorine to react with metals to form very stable metal fluorides. In this report, we describe the results of experiments in which metal scrubbers were used to selectively remove F_2 from a mixture of F_2/NF_3/ Rare gas.

B. APPROACH

The reactor consists of a stainless steel cell containing either Ni or Ti metal which can be heated to various temperatures. Mixtures containing F_2 and/or NF_3 and a rare gas buffer (He or Ar) are circulated through the reactor and are continuously monitored using a mass spectrometer (Model 100C, U.T.I., Sunnyvale, CA). A photograph of the apparatus is shown in Figure 2 and a schematic diagram is shown in Figure 3.

Premixed gas is introduced into the flow loop with the reactor valves (V2 and V3) closed and the bypass valve (V1) open. A circulating pump is used to pump the gas at a flow rate of typically 6 /min as monitored by a linear mass flow meter (Teledyne-Hastings, Hampton VA, Model H-10KMS).

Before the valves to the reactor are opened to start an experiment, the mass peaks monitored by the mass spectrometer [m/e (F_2) = 38; m/e (NF_3) = 71, m/e (Ar) = 40] show essentially no change. At the beginning of an experiment, the bypass valve is closed and the two valves connecting the metal reactor are opened. After a transient spike caused by pressure equalization, the mass spectrometer monitors the decay of the fluorine containing species as a function of time. A typical decay curve for F_2 flowing through a Ni filled reactor at 300^{o}C is shown in Figure 4. In this case a mixture of 5% F_2 and 95% He at a total pressure of 128 torr was used. An exponential decay over

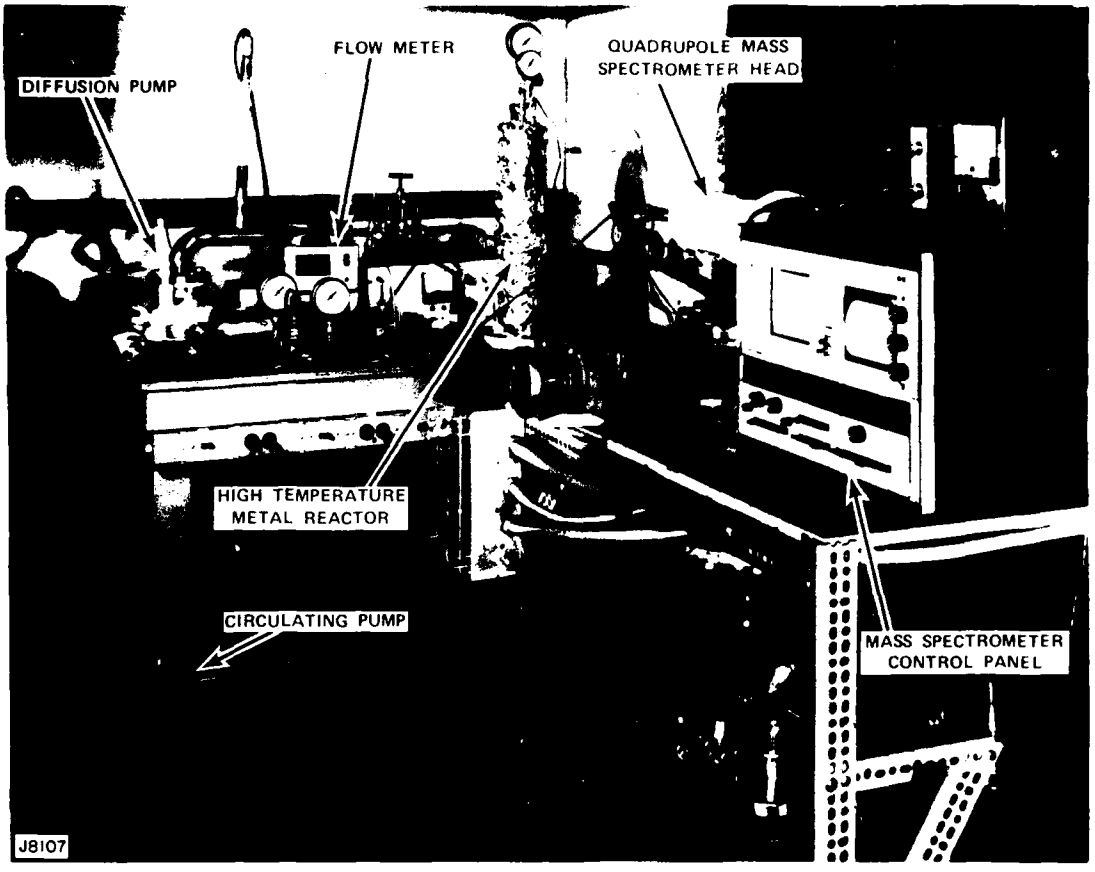

Figure 2 Photograph of the Gas Scrubbing Apparatus

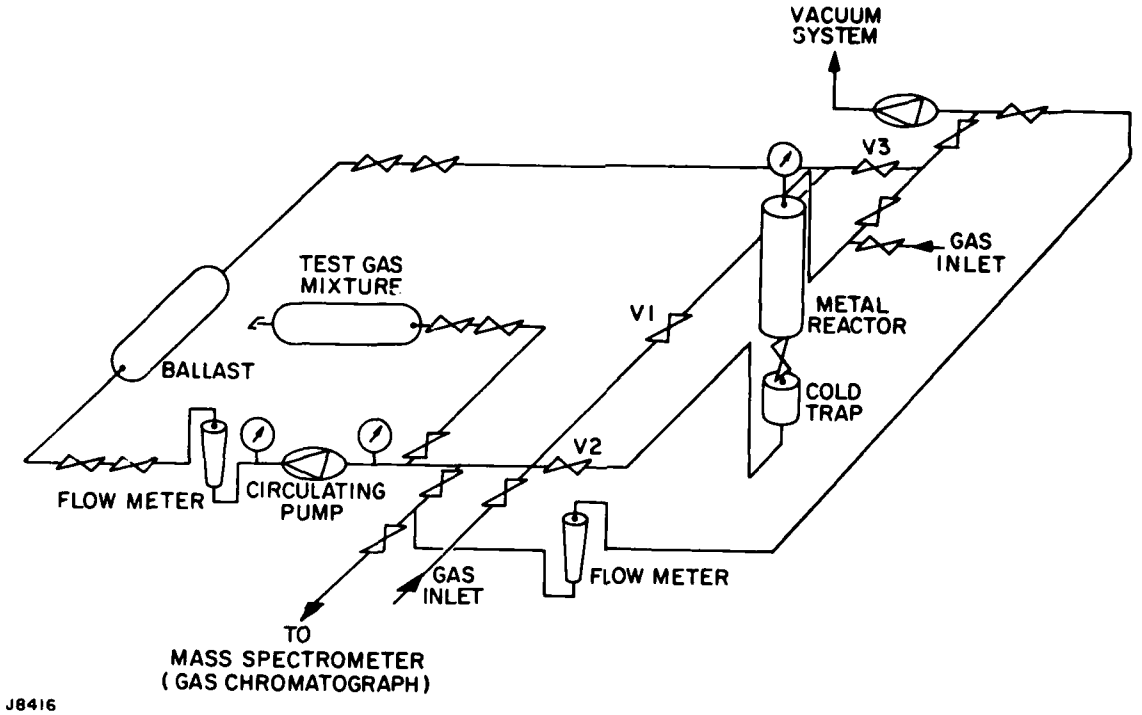

Figure 3 Schematic Diagram of Gas Scrubbing Apparatus

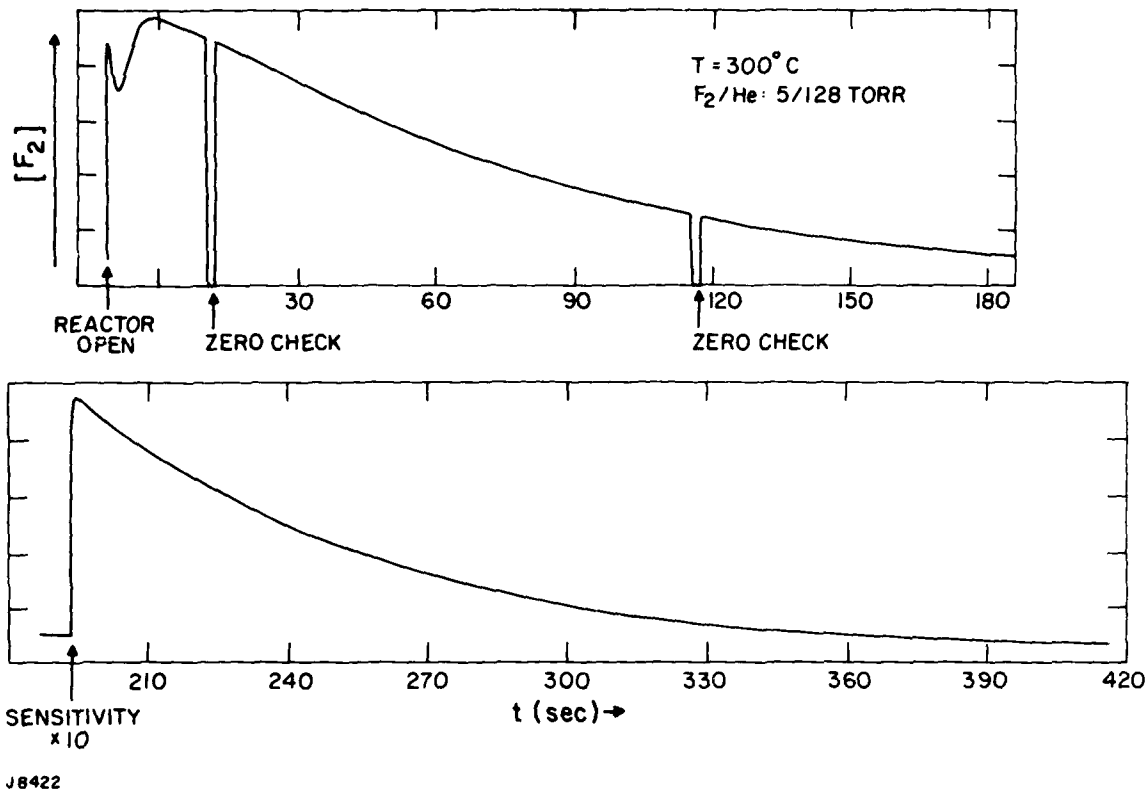

Figure 4 Time Dependence of F_2 Loss in a Nickel Filled Reactor at 300°C

about two orders of magnitude is observed with a decay time constant of about 80 sec. In other experiments, the nickel is replaced with a different metal to be tested, e.g., the decay time constant for F_2 in a Ti reactor is significantly faster even at lower temperatures. A typical decay of F_2 in Ti is plotted in Figure 5 together with the system response time.

For our application, we are interested in scrubbing the F_2, i.e., separating F_2 from NF_3. It is, therefore, important to determine the rate of decay of NF_3 under similar conditions to determine if one can remove F_2 in the presence of NF_3 or if the halogens must be removed together. A plot of the NF_3 decay versus time in a Ti reactor at 180°C is given in Figure 6. We observe about a two order of magnitude difference in the decay rates of F_2 and NF_3 under similar conditions. This suggests that by limiting the contact time a selective mode can be achieved and F_2 removed from a typical laser mixture.

C. DATA AND DISCUSSION

A series of measurements of the decay rates of both F_2 and NF_3 in a Ti filled reactor has been performed as a function of temperature. As has already been shown in Figures 5 and 6, however, the reaction rates of NF_3 and F_2 in a Ti reactor at 180°C are substantially different. If we now compare the decay rates as a function of temperature as given in Figure 7, we observe that the F_2 rate is substantially higher for all temperatures up to 180°C. Thus, Ti can be used effectively to eliminate F_2 from a mixture containing F_2 and NF_3. It should be noted that measurements of F_2 removal in a Ti filled reactor were made above 180°C but the rates were comparable to or greater than the system response time and could not be determined.

For comparision, Figure 8 shows the decay rates of F_2 and NF_3 in a Ni filled reactor. Since both the activation energy and the reaction rates for the decay of F_2 and NF_3 in a Ni

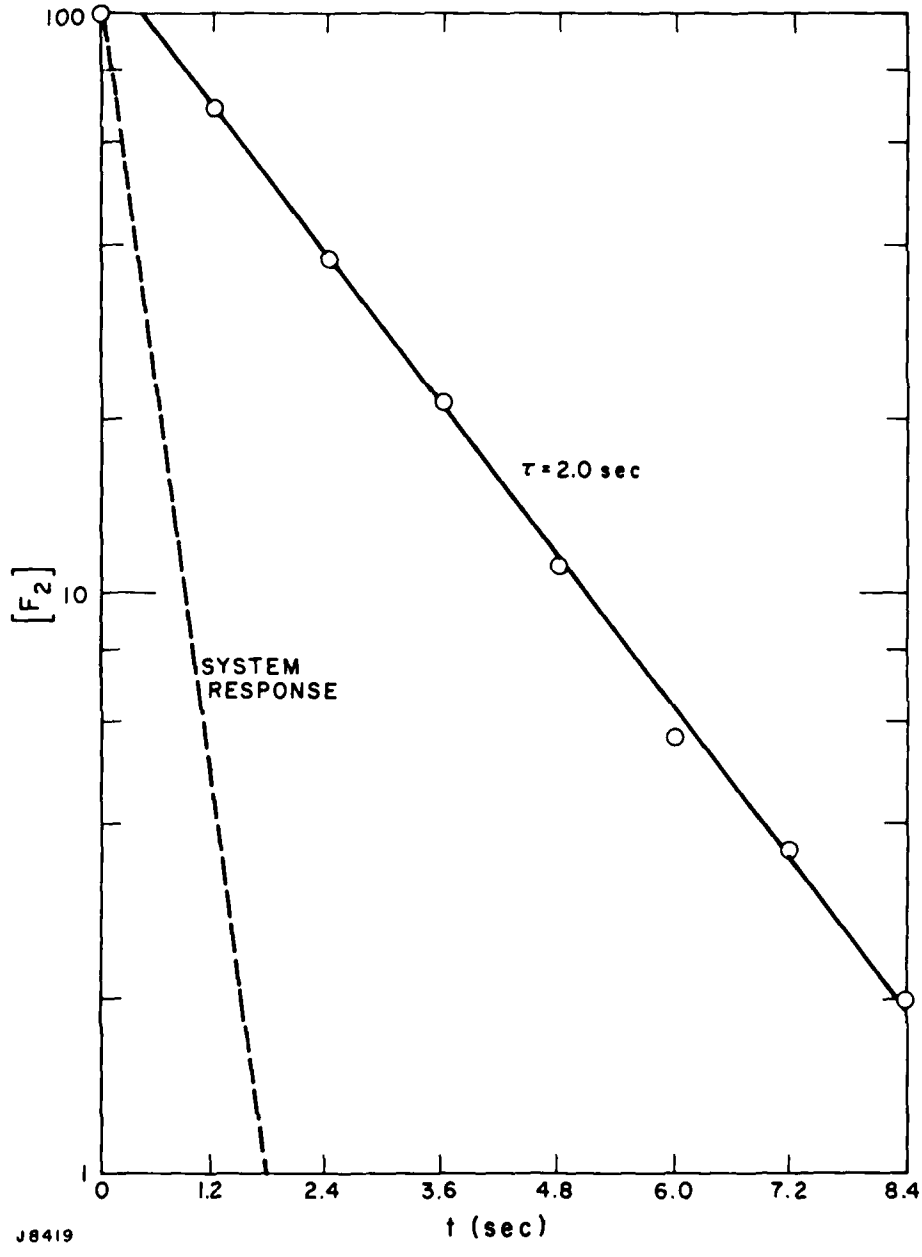

Figure 5 Semilog Plot of Time Dependent F_2 Loss in a Titanium Filled Reactor at 180°C

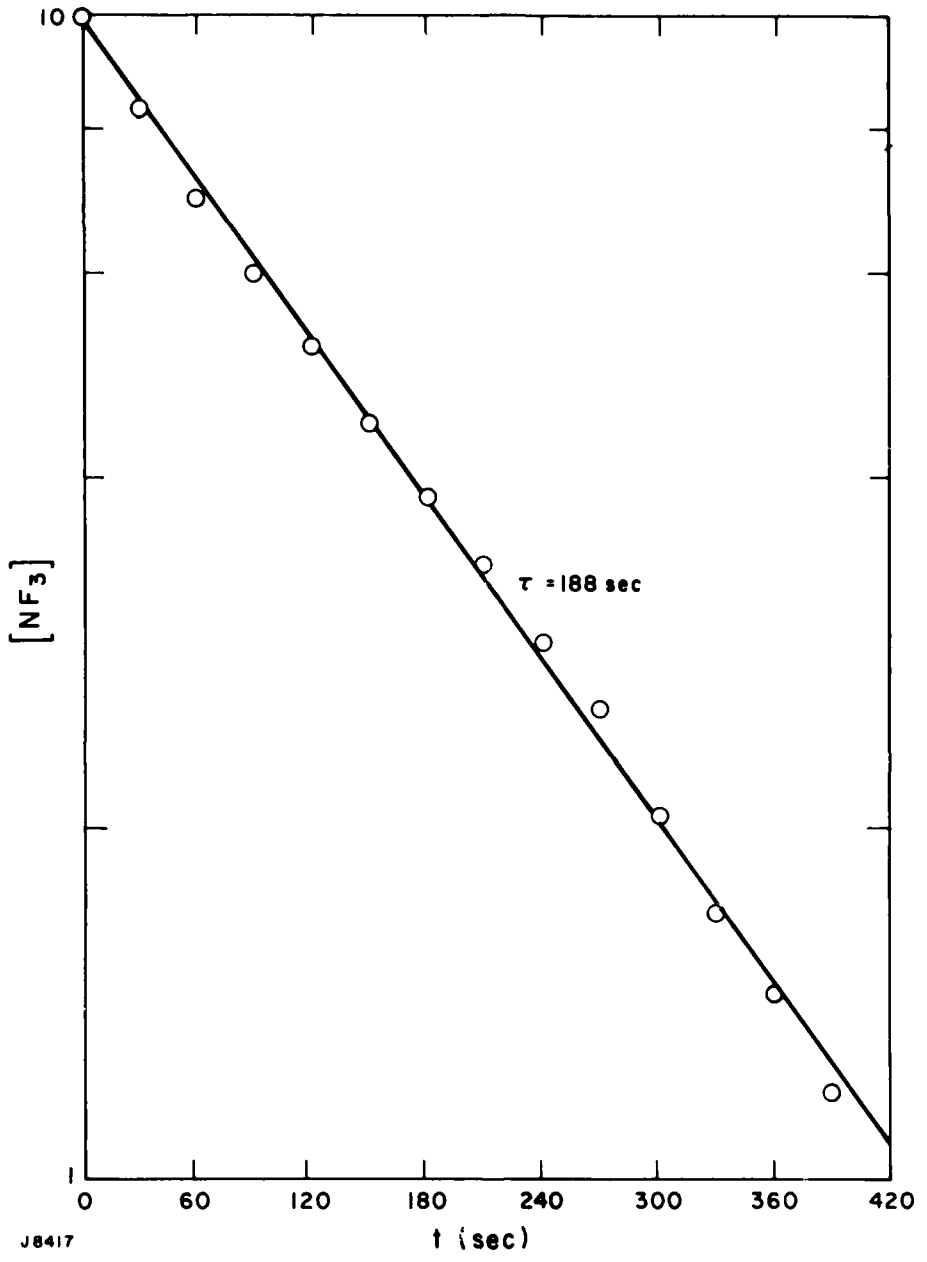

Figure 6 Semilog Plot of Time Dependent NF_3 Loss in a Titanium Filled Reactor at 180°C

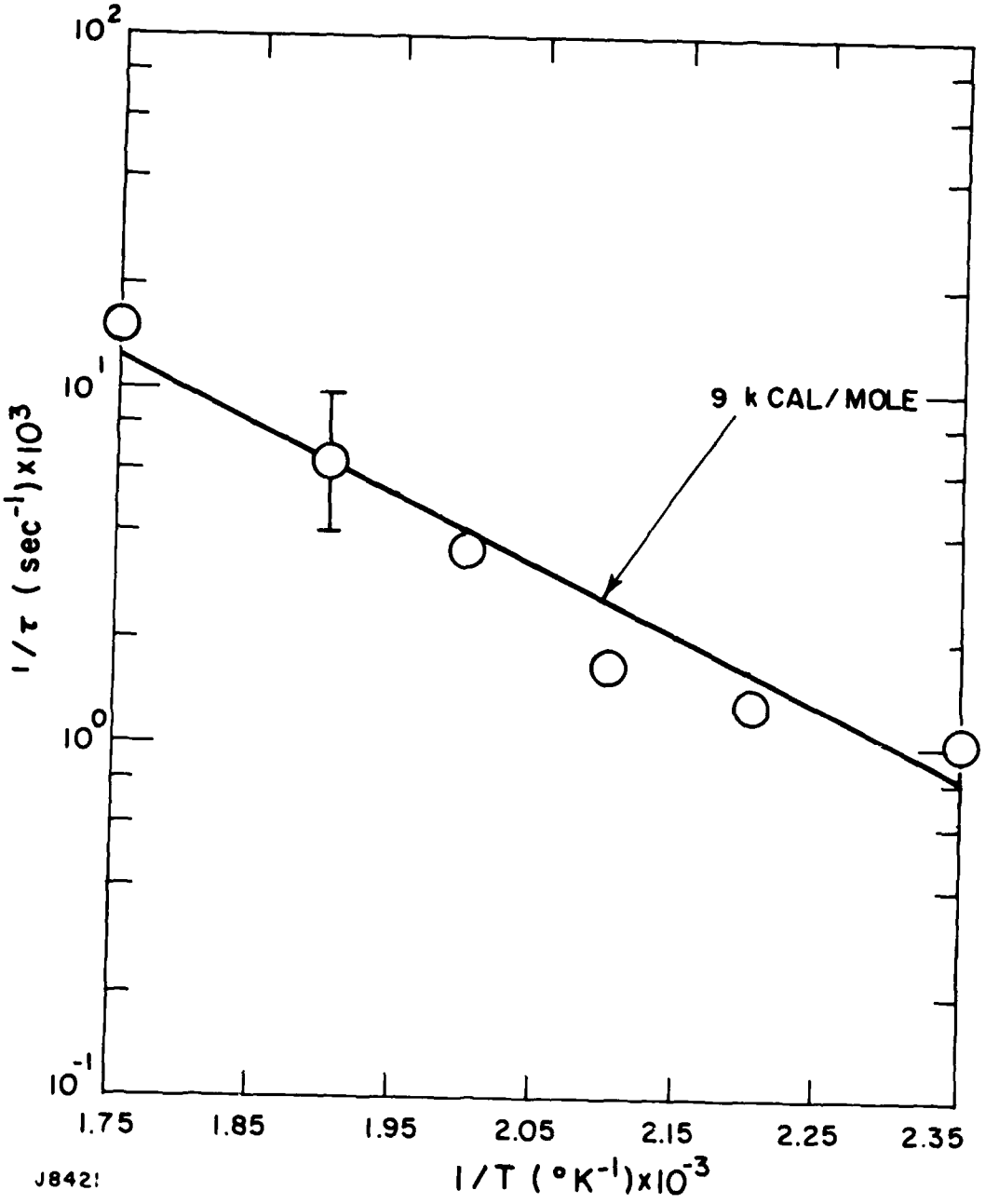

Figure 7a Temperature Dependence of F_2 Loss Rate in a Nickel Filled Reactor

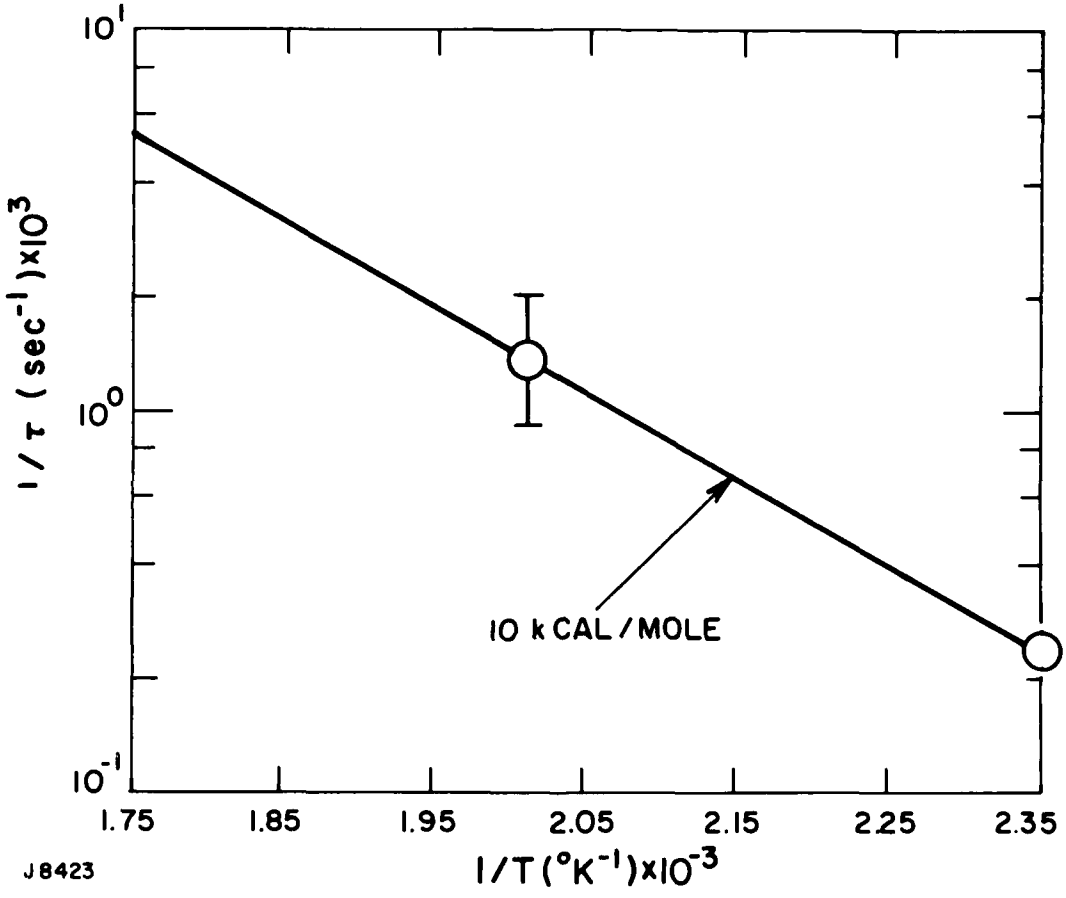

Figure 7b Temperature Dependence of NF_3 Loss Rate in a Nickel Filled Reactor

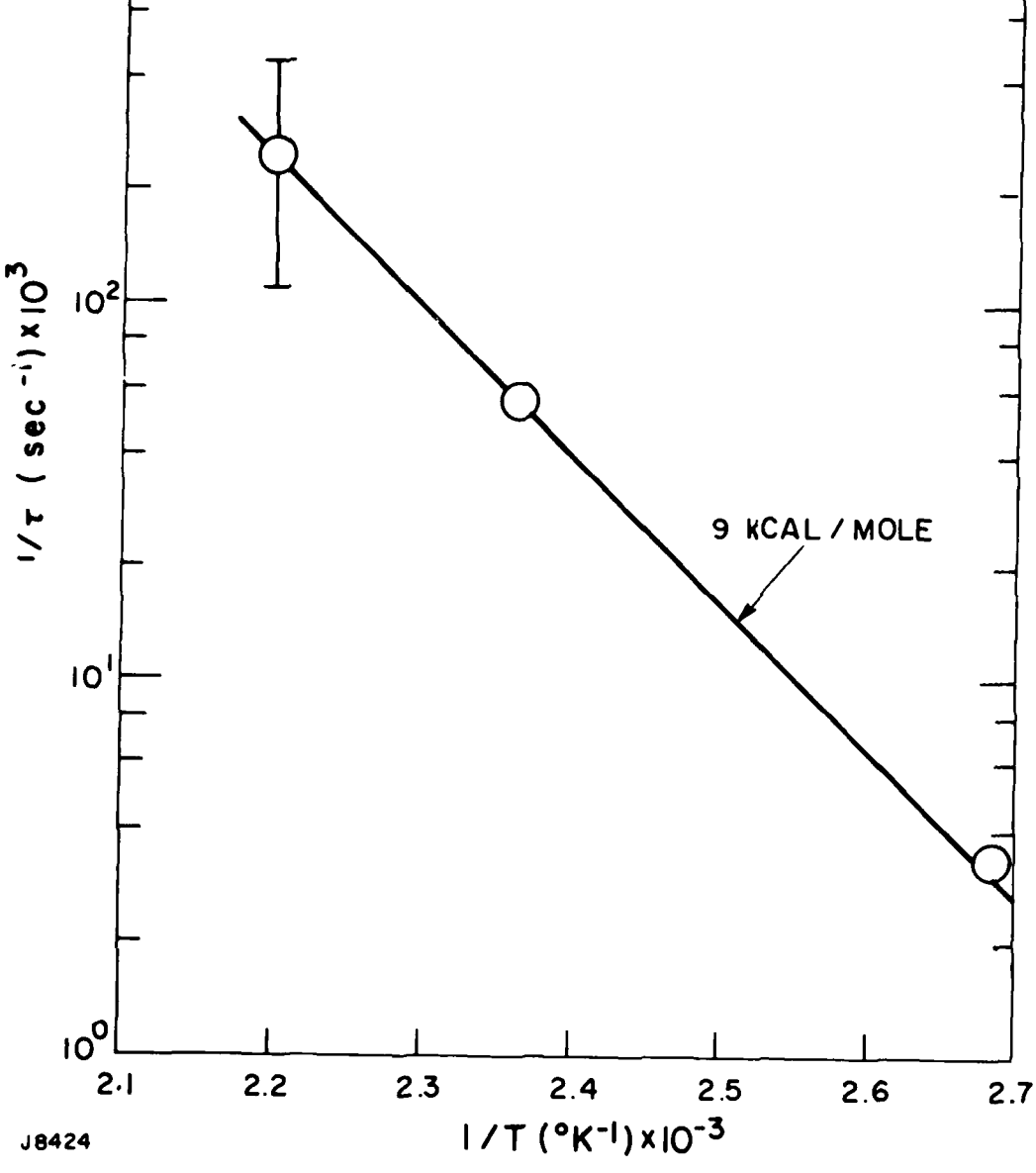

Figure 8a Temperature Dependence of F_2 Loss Rate in a Titanium Filled Reactor

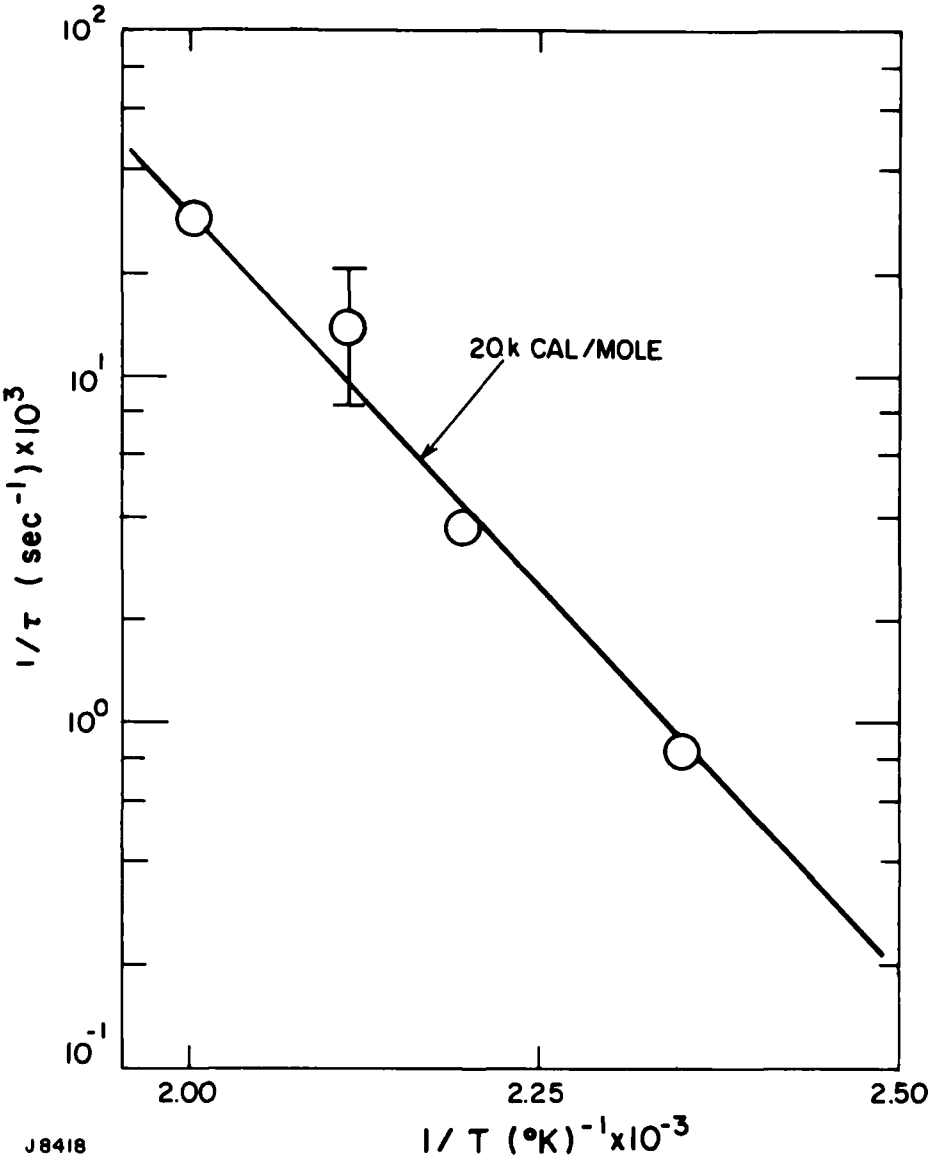

Figure 8b Temperature Dependence of NF_3 Loss Rate in a Titanium Filled Reactor

filled reactor are comparable, there is no temperature at which preferential scrubbing of F_2 from the mixture can be easily accomplished.

The error bars in Figures 7 and 8 represent standard deviations about the mean of a set of decay rate measurements obtained at each temperature. The mean is represented by an individual data point (open circle). Some component of this error is not random, but rather is due to a systematic slowing down of the rate as material is processed in the reactor, i.e., passivation of the reacting material. For any particular measurement of the temperature dependence, however, the activation energy remains relatively constant, especially at the higher temperatures. Also, the average of the runs gives the same activation energy.

An interesting difference between Ni and Ti reactors is that the reaction products in a Ni reactor form nickel fluorides which have low vapor pressures at the reactor temperatures. Thus, the surface becomes coated with nickel fluorides which can substantially slow the reaction rate. Nickel fluorides in the form of a green powder have been observed to form in the Ni reactor. On the other hand, Ti reaction with fluorine forms TiF_4 which is a volatile gas at the reactor temperature (vapor pressure ~ 10's of torr).

This gas is trapped as it emerges from the reactor (see Figure 3) and forms a white powder on a cold trap surface. At present, it is not clear whether the difference in vapor pressures of the metal fluoride products plays an important role in determining the net decay rates measured here.

D. CONCLUSIONS

A Ti reactor has been used previously in a closed-cycle recirculating system for a rare-gas halide excimer laser.[11]

(11) Johnson, P. M., Keller, N. and Turner, R. E., Appl. Phys. Lett. 32, 291 (1978).

In that case, the laser mixture consisted of only F_2 and a rare gas. In our case, we are removing fluorine from a mixture containing both F_2 and NF_3 in a rare gas. For the Ti reactor we have shown selective removal of F_2 in the presence of NF_3 with a rate which is about two orders of magnitude faster than the NF_3 removal rate.

In the Ti reactor, TiF_4 forms and is trapped downstream so that the Ti surface is self-cleaning and one should be able to use up a significant fraction of the Ti charge before it must be replaced. Each Ti atom reacts with four fluorine atoms so that for every mole of F_2 removed from the gas stream a half mole of Ti or about 24 g is consumed.

The rate at which gas must be processed in a closed-cycle XeF laser will be determined by the rate at which F_2 is formed. This rate can be estimated by the limited knowledge of the gas phase kinetics but little is known about the total reaction rate at high temperatures and pressures. Thus, if it takes N pulses before the XeF laser output decreases to an unacceptable level, one would have to process 1/N fraction of the gas on each cycle.

III. MATERIALS COMPATIBILITY STUDIES

A. INTRODUCTION

The objective of this task is to investigate the reactivity and compatibility of some constituents of heated XeF laser gas mixes (namely, gas phase NF_3 and NF_2) with a number of structural materials that may be considered for the design of high-power, closed-cycle, efficient XeF laser systems. These fluorine-bearing constituents were chosen because they are the dominant reactive species in the XeF laser mix. NF_3 is the primary halogen donor, and NF_2 is one of the principal reaction products formed in the homogeneous gas phase chemistry that follows e-beam excitation of neon/xenon/NF_3 gas mixes. The structural materials (e.g., stainless steel, copper, aluminum and quartz) were chosen as being representative of the types of materials from which heat exchangers, duct work, mufflers, foils, laser cavities, and optics are constructed. Furthermore, these studies were performed at elevated temperatures (up to 500^{o}K), to include the temperature range at which the XeF laser electrical efficiency is optimized.

In general, material compatibility studies provide input information that can be used to assist in determing a number of important laser design parameters. First, the heterogeneous and homogeneous NF_3 reaction rates determine the total NF_3 lifetime around the closed-cycle flow loop. This, in turn, determines the NF_3 makeup rate required to maintain the proper NF_3 density within the laser cavity. At the inception of this work, quantitative NF_3/surface reaction rates were not available although some information regarding homogeneous NF_3 loss rates is now becoming available. Second, a knowledge of NF_x/surface reaction products and rates determine whether or not gas scrubbers

are required for a given run time, the size and type of scrubbers needed and the fraction of the flow that should be processed. In addition, product identification may aid in determining the existence of unwanted absorbers or other species that interfere with upper laser state formation or increase quenching losses especially if these products are highly volatile. Third, the NF_x/ surface reaction rates determine (at least indirectly), the corrosion rate and overall lifetime of the various components of the flow loop that are in contact with the hot laser gas mix.

In the present studies, we have measured the rate of loss of NF_3 and NF_2 in the presence of various metals and quartz at elevated temperatures. The NF_2 loss rate was monitored by an optical absorption technique and the NF_3 loss rate was monitored using mass spectrometry. These diagnostics also provided some qualitative information pertaining to surface reaction products.

Several caveats should be mentioned in regard to interpreting the results presented below. The NF_3 and NF_2 loss rates reported here pertain to specific samples of metal or quartz, and may not be generally applicable to other arbitrary metal or quartz samples of the same material. The reason for this rather conservative interpretation of the data stems from the variability in experimental measurements of surface reaction rates. This variability is associated with difficulties in characterizing and controlling parameters such as surface treatment (especially surface roughness and impurities) and bulk material structure (dislocations and other defects, bulk impurities) which can have a significant impact on surface reaction rates. This situation could be rectified if a sufficient amount of data is obtained over a wide range of sample variations (surface and bulk morphology, alloy composition, sample size and shape, etc.) for each particular material, but this was outside the scope of this program.

B. BACKGROUND

During the early stages of the program, a literature search was undertaken to obtain information regarding the homogeneous and

heterogeneous chemistry relevant to NF_3/NF_2 laser compatibility. This study produced a number of references which were extremely useful source materials.[12-14] Among these, Ref. 14 was particularly useful as it contains a two-volume, exhaustive compilation of chemical and engineering data on NF_3. Part A contains evaluated data on the chemical, physical and thermodynamic properties of NF_3. It also contains engineering data related to the storage, handling, toxicology, production and corrosion rates of NF_3 with various materials. Part B is an extensive bibliography containing more than 5000 citations concerning NF_3 properties. In what follows we briefly summarize a few of the salient features of NF_3 and NF_2 chemistry that bear on the present program. All of this information was obtained from the three references cited above.

1. Homogeneous Chemistry

At high temperature and in the absence of walls, NF_3 thermally dissociates in an argon bath into the difluoroamino radical, NF_2, and a fluorine atom via the bond fission reaction (3):

$$NF_3 + Ar \rightarrow NF_2 + Ar + F \qquad (3)$$

(12) Hoffman, C.J., and Neville, R.G., Chem. Rev. 62, 1 (1962).

(13) Colburn, C.B., in "Advances in Fluorine Chemistry", ed., Stacey, M., Tatlow, J.C., and Sharpe, A.G., Vol. III, Butterworths, Washington, D.C. (1962).

(14) Anderson, R.E., Vander Wall, E.M., and Schaplowsky, R.K., USAF Propellant Handbooks, Vol, III, Part A: Nitrogen Trifluoride Systems Design Critera; Part B: Nitrogen Trifluoride Bibliography.

Subsequent chemistry involves only the recombination of the F atoms

$$F + F + Ar \rightarrow F_2 + Ar \quad (4)$$

and the two-body recombination of NF_2 radicals

$$NF_2 + NF_2 \rightleftarrows N_2F_4 \quad (5)$$

The rate constant for the homogeneous thermal decomposition of NF_3 in argon, reaction (3), has been measured in shock tube studies at higher temperatures (1050-2400°K) than would be encountered in an XeF laser.[15-18] The total pressure range in these studies was 0.4-60 atm of which NF_3 constituted only a few percent concentration in the mix. In all cases the rate was found to be first order in both Ar and NF_3 concentration and the rate constant was expressed in the form:

$$k_1(T) = Ae^{-E_a/RT}$$

The results of these studies are summarized in Table 1. The agreement between the data in Refs. 15, 16, and 18 is reasonably good, but the discrepancy between these data and that of Ref. 17 is unresolved. Extrapolating the data in Table 1 down to 500°K, we find that the homogeneous process should play a negligible role in determining the overall NF_3 loss rate in the presence of metals and quartz as measured in Section III.D.3.[15-18]

(15) "Quarterly Progress Report on Physical Chemistry", Rept. No. 63-25, Rohm and Haas Co., Huntsville, Ala., Contracts DA01-021-ORD-11878 and -11879, Sept. 4, 1964.

(16) MacFadden, K.O., and Tschuikow-Roux, E., J. Phys. Chem. 77, 1475 (1973).

(17) Dorko, E.A., Grimm, U.W., Scheller, K., Mueller, G.W., J. Chem. Phys. 63, 3596 (1975).

(18) Evans, P.J., and Tschuikow-Roux, E., J. Chem. Phys. 65, 4202 (1976).

TABLE 1. BIMOLECULAR RATE CONSTANTS FOR NF_3 THERMAL DISSOCIATION

$A(cm^3/sec) \times 10^{10}$	E_a(kJ/mole)	P(atm)	T (^oK)	Ref
5.6	146.7	0.3-2.4	1100-1450	15
2.09	125.8	2.7-6.0	1050-1390	16
8.3	235	0.8-60	1500-2400	17
677.	200.6	0.8-1.81	1150-1530	18

The rate constant for the reversible dimerization reaction has been measured over the temperature range 344°K-571°K and the pressure range 0.6 - 6 atm.[19] These results indicate that the equilibration in Eq. (5) is rapidly established (milliseconds or less) for the temperature range of interest to XeF lasers. The fractional dissociation, $\alpha(= NF_2/N_2F_4)$, calculated from thermodynamics is 0.004 at 1 atm and 0.12 at 10^{-3} atm at 298°K and the corresponding values at 423°K are 0.9 and 0.94, respectively.

2. Heterogeneous Chemistry

The heterogeneous reaction of NF_3 with metals at elevated temperatures has been the subject of a large number of studies.[20-23] Colburn and Kennedy[20] reported that N_2F_4 was produced by heating NF_3 in a metal-filled reactor via the overall reaction

$$2NF_3 + 2M \rightarrow N_2F_4 + 2MF \qquad (6)$$

over the temperature range 375-450°C. Here M is any of a number of various metals (stainless steel, copper, arsenic, antimony, bismuth) that were studied in those investigations.[20] Much of this early work utilized copper that promoted the reaction by the

(19) Brown, L.M., and Darwent, B. de B., J. Chem. Phys. 42, 2158 (1965).

(20) Colburn, C.B., and Kennedy, A., J. Amer. Chem. Soc. 80, 5004 (1958).

(21) Gould, J.R., Corey, H.S., Schuhlein, F.T., and Smith, R.A., "High Energy Monopropellants, Rept. No. SCC-26-QPR-5, Stauffer Chemical Co., Contract NOas 58-667-C, Sept. 1958.

(22) Cohen, M.S., "N-F Research and Development at Reaction Motors", Reaction Motors Division, Thiokol Chem. Corp. paper presented at Second N-F Chemistry Symposium sponsored by ONR, Dec. 1959.

(23) Francis, W., "The Preparation of Nitrogen Trifluoride and Tetrafluorohydrazine", ibid, 1959.

formation of CuF (or CuF_2). The N_2F_4 formation mechanism involves, initially, NF_3 attack on virgin metal forming a stable metal fluoride via

$$NF_3 + Cu \rightarrow CuF + NF_2 \qquad (7)$$

and then N_2F_4 is formed via NF_2 dimerization as the reactor cools.

Following these studies,[20] other work sought to improve reaction yields..[21-23] Given this proposed mechanism, most of these improvements were directed towards replacing copper with another substance that would generate a volatile metal fluoride and, therefore, provide a continuous exposure of fresh metal to NF_3. In this regard carbon (yielding CF_4 (b.p. = -127.7°C)) and arsenic (yielding AsF_3 (b.p. = 56.3°C)) were extensively studied with varying degrees of success.

C. APPARATUS

Under this program, we initially anticipated using a UV optical absorption diagnostic and a mass spectrometer to monitor the F_2 scrubbing (Task II) and materials compatibility (Task I) experiments, respectively. However, during the early phases of Task I, we encountered difficulties in the determination of the NF_3 loss rate with metals using the optical diagnostics. These difficulties were found to be related to the presence of interfering species including other NF_x type compounds which also absorb at the NF_3 probe wavelength of 193 nm, and which are formed in the NF_3/metal decomposition reactions. On the other hand, no such difficulty was encountered in the NF_2 compatibility experiments. Rather than attempt to extract the pure NF_3 absorption signal, it was decided that mass spectroscopy could be used to perform the NF_3 compatibility experiments by unambiguously monitoring the NF_3 loss rate using the m/e = 71, NF_3^+, mass spectrometer signal.

In what follows below, we describe the optical absorption apparatus that was used to monitor NF_2 materials compatibility experiments. A description of the NF_3 materials compatibility apparatus is to be found in Secton II.B.

A schematic diagram of the optical absorption apparatus is displayed in Figure 9 and a photograph of the entire apparatus is displayed in Figure 10. Basically, UV light emanating from a cw D_2 lamp was attenuated by a heated gas cell containing NF_2 and an appropriate metal. NF_2 absorbs around 260 nm. The transmitted light was then spectrally resolved and detected by a 0.3 m (GCA/McPherson Model 218) vacuum monochromator and photomultiplier tube (EMI/GENCOM MODEL 9789Q, spectrasil UV grade window). The modulated output of the photomultiplier was fed into a lock-in amplifier (PAR Model 120), and the lock-in output was displayed on one channel of a strip chart recorder. 43 Hz modulation was obtained by a mechanical chopper wheel (Ithaco Corp.) inserted between the light source and cell. The chopper also outputs a synchronous 43 Hz square wave electrical signal that was used to provide phase reference for the lock-in amplifier. An optical reference signal (used for normalization) was obtained by reflecting a small portion of the incident UV beam on to the surface of a glass slide covered with a thin layer of sodium salicylate solution. The resultant visible fluorescence was detected with a 1P28 photomultiplier tube, the output of which was fed into a second lock-in amplifier for display on the second channel of the strip chart recorder.

The D_2 arc lamp (Oriel Corp. Model 6311) emitted continuum radiation from $\sim$185 nm to 490 nm, the short wavelength limit being determined by the transmission characteristics of the quartz lamp envelope. The lamp output was collimated with a UV grade quartz f/1.5 condensing lens positioned about one focal length ($\sim$4 cm) from the lamp envelope. The light then passed through two variable size apertures, which defined the probe volume within the gas

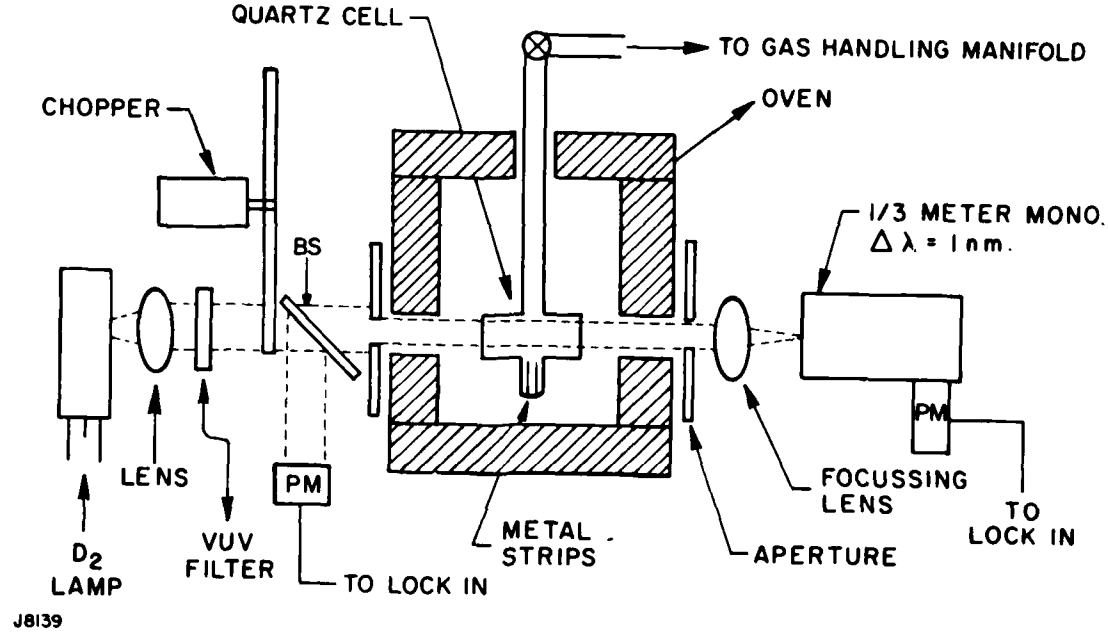

Figure 9 Schematic Diagram of NF_2 Materials Compatibility Experiment

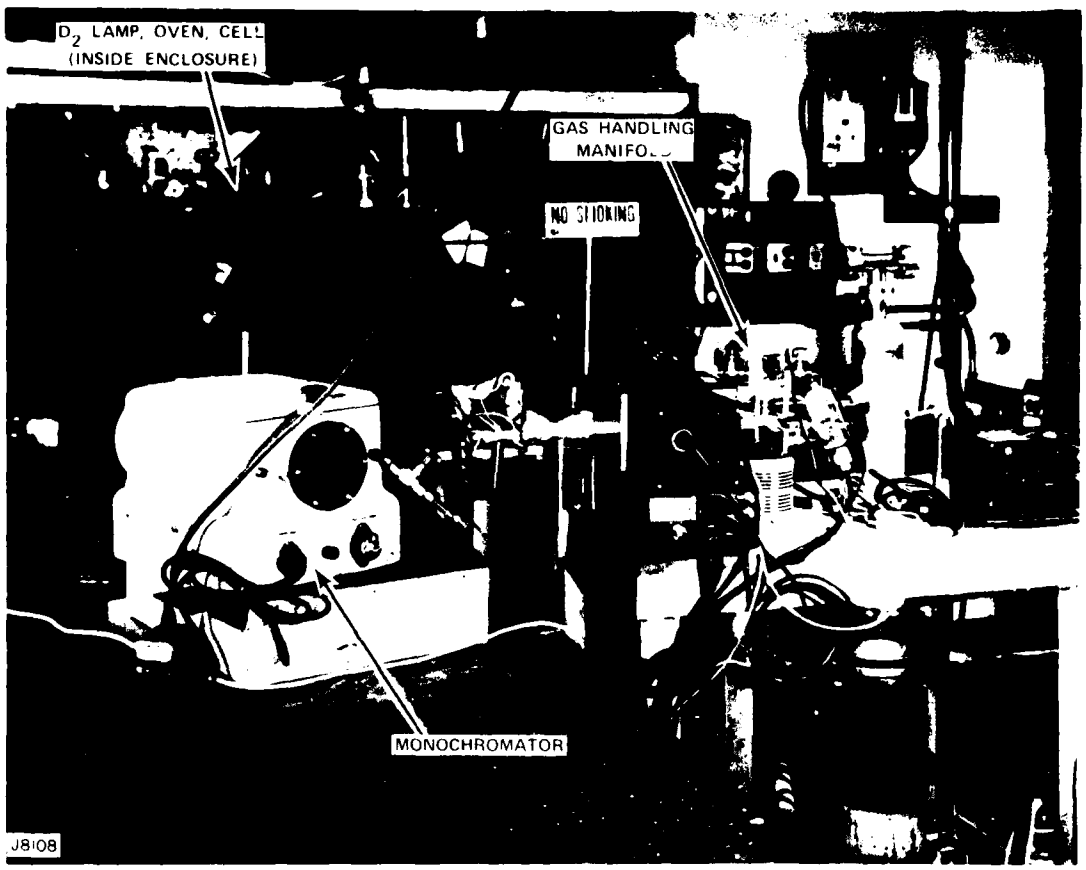

Figure 10 Photograph of Material Compatibility Experiment

cell, before entering the monochromator. The monochromator bandwidth ($\Delta\lambda \simeq 1$ nm) and wavelength calibration were determined using a low pressure Hg resonance lamp. An additional dielectrically coated interference filter (Acton Corp., $\lambda_{max} = 172$ nm $\Delta\lambda \simeq$ 20 nm) was inserted into the UV beam path when NF_3 probe experiments at 193 nm were performed.

The gas cell was constructed entirely from suprasil quartz. This was done in order to insure that hot NF_2 gas was in contact with metal at one controlled location which was within a finger-like compartment appended to the cell body. The cell was constructed by fusing two optical quality 2.54 cm diameter windows to either end of a 2.54 cm diameter x 10 cm long tube. A long combination gas inlet and vacuum pumping line (30 cm x 0.6 cm diameter) and the finger-like compartment were also fused to the cell body. The long inlet line passed through a hole in the oven wall and mated to the stainless steel vacuum station via a 0.6 cm quick disconnect coupling. The ambient temperature at this junction was always near room temperature.

The gas cell was enclosed within oven walls constructed entirely of firebrick and transite. Small holes drilled into the oven walls allowed the UV probe beam to enter and exit the cell. The oven was resistively heated using Nichrome heaters which were powered by a variac transformer. The Nichrome heaters were located on the floor of the oven. The cell temperature was controlled to within $10^{o}K$ by means of a thermocouple control relay circuit. The cell temperature was monitored at two positions: the bottom of the finger and the top of the cell. These two readings were always within $10^{o}K$ of each other.

The stainless steel vacuum station and gas handling manifold (see Figure 10) were used to evacuate the gas cell, make NF_2/argon mixes and load gas samples into the cell. The base pressure of the vacuum station and heated cell ($500^{o}K$) was about 1×10^{-6} torr and the net outgassing/leak rate (with the cell <u>hot</u>) was $\sim 1 \times 10^{-3}$ torr/min in a volume of about 200 cm^3.

Vacuum measurements were made with a Bayard-Alpert type (Vecco Corp. Model RG7) ionization gauge, and gas pressures were measured with a calibrated pressure transducer (Validyne Corp. variable reluctance manometer Model DP7).

Samples of NF_3 and N_2F_4 were obtained from Air Products Corp. N_2 was removed from both gases by trapping and pumping at 77°K. In addition, NF_3 samples were trapped in dry ice/acetone slush baths (190°K) to remove water vapor and NO_2.

D. RESULTS

The rate of NF_2 loss was followed by time resolved UV absorption at 260 nm, the peak of the strong A → X bound-bound absorption band in NF_2.

1. NF_2 UV Absorption Cross Section

The NF_2 optical absorption cross section was measured at 260 nm. The data displayed in Figure 11 were obtained at 500°K using a 3l/l argon:NF_2 mix. The absorption cross section was then obtained from the slope of a straight line drawn through the data points using the relationship.

$$\sigma = \frac{1}{N\ell} \left[\ell n(I_o/I)\right] \qquad (8)$$

where ℓ is the optical path length (= 9 cm) and N is the NF_2 density. Using Eq. (8), the cross section was calculated to be 1.3×10^{-18} cm^2 at 500°K, which is somewhat larger than the room temperature value, 9.2×10^{-19} cm^2, measured by other workers.[24] In addition, relative measurements were made at a few wavelengths on either side of absorption maximum in order to verify that NF_2 was the principal absorber in this wavelength region. The resultant continuous absorption curve was characteristic of NF_2.

(24) Markeev, G.N., Sinyanskii, V.F., Smirnov, B.M., Doklady Akademic Nauk SSSR 222, 151 (1978).

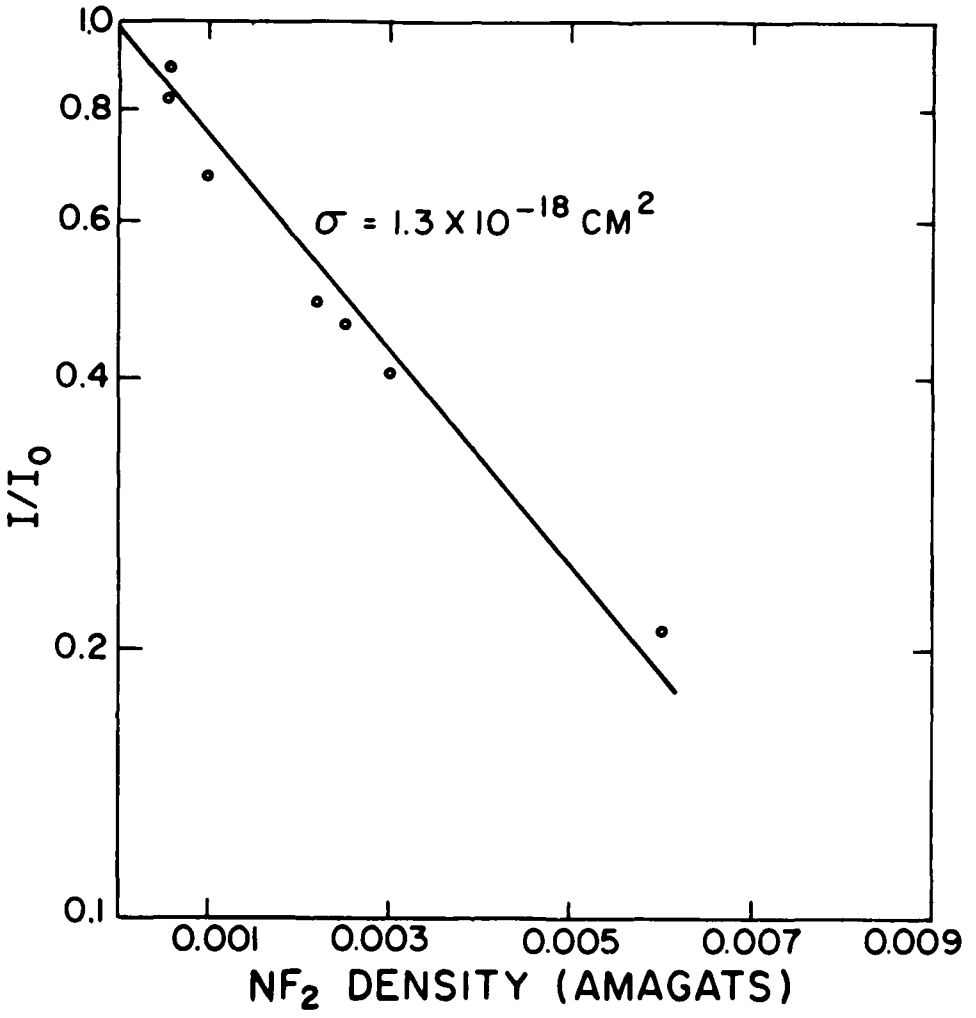

J9526

Figure 11 NF_2 Absorption Cross Section Data at 500°K

2. NF_2 Loss Rates

The NF_2 loss rates were measured for hot NF_2 gas in contact with the following materials: quartz, 304 stainless steel, nickel, 6061 aluminum, copper and platinum. The quartz experiments provide a reference measurement with which to compare the loss rates measured with metals added to the quartz cell.

A standardized handling and data taking procedure was adopted in order to minimize systematic errors and to provide meaningful comparisons between data obtained using the different metals. Except for platinum, the metal specimens were each chosen to be eight strips of foil with surface area comparable to the surface area of the quartz cell. In the case of platinum a smaller area of foil was used. All metal pieces were cleansed with an acetone wash to remove organic surface impurities. Prior to taking data, the cell and metal specimens were baked and pumped at $500^{\circ}K$ at 10^{-6} torr for ~ 2 hr.

Three loss rates were measured for each metal using a 31 to 1 argon/NF_2 mix containing 2.3×10^{-3} amagats NF_2. This density yields about 50% absorption at 260 nm in a 9 cm cell. The first loss rate was obtained for a mix in contact with virgin metal while the second and third loss rates were obtained after the same metal sample had been exposed to high concentation NF_2 samples (0.16 amagats pure NF_2) for 15 and 30 min periods, respectively. This procedure provided a means to assess the effects of passivation. The passivating samples were added between the first and second loss rate measurement and then again between the second and third loss rate measurement. The NF_2 concentrations quoted here were obtained from N_2F_4 pressure measurements at room temperature using the ideal gas law and thermodynamic calculations which show that N_2F_4 is totally dissociated at $500^{\circ}K$.

A typical time dependent NF_2 absorption curve is displayed in Figure 12 for 304 stainless steel. The absorption increased

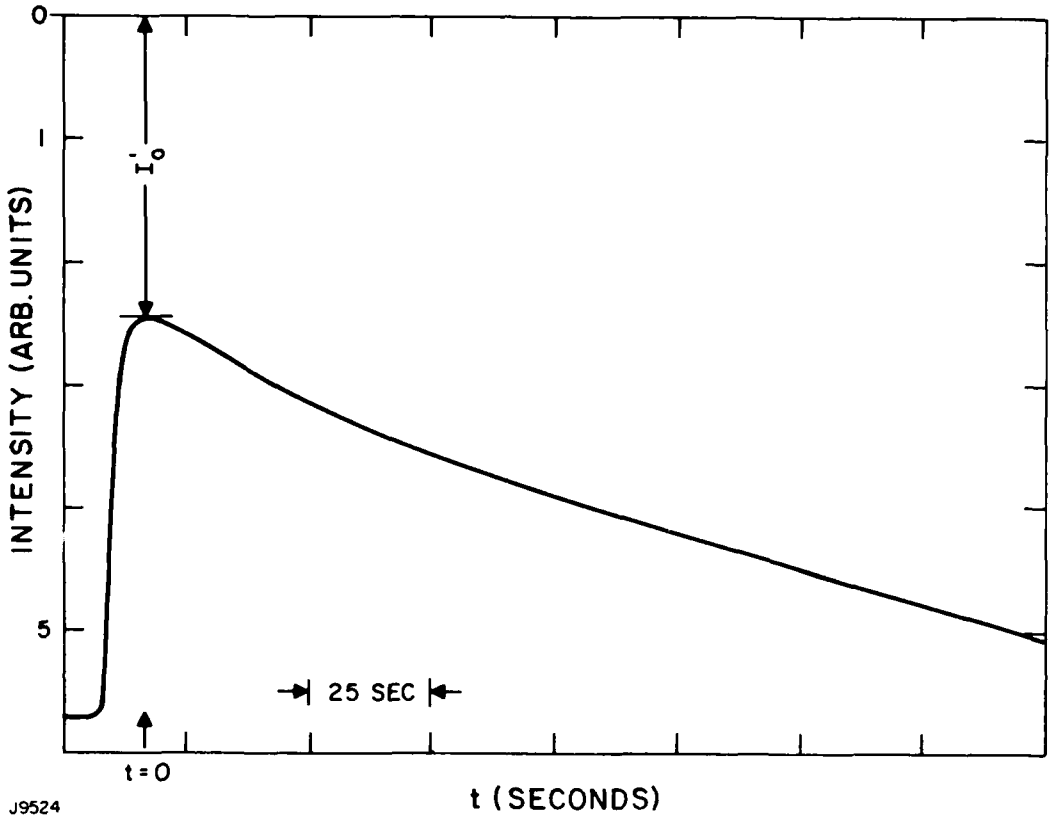

Figure 12 Time Dependence of NF_2 Signal

initially as the NF_2/argon gas mix enters the cell. This is followed by a steady decrease in absorption (or transmission increase) as NF_2 molecules are removed from the probe volume within the cell. For comparison, the baseline measurement (see Figure 13) using only the quartz cell indicates a much slower decay rate under nominally identical conditions. The faster decay rate observed with metal present in the cell is indicative of a chemical reaction between NF_2 and metal; the fact that the loss rate depends upon the presence of metal eliminates the possibility that mass transport effects could cause the apparent loss of NF_2. It is likely that the reaction involves the formation of metal fluoride compounds in a manner analogous to NF_3/metal reactions discussed earlier (see Background). It is also worth noting that the curve shape in Figure 12 suggests that the NF_2/metal reaction is initiated as soon as the gas contacts the metal. Otherwise, a flat plateau (or induction period) would have been observed between the rise and fall times. These observations were found to be generally true for all the metals investigated here.

In all cases, the decaying portion of the absorption curves was found to fit a single exponential functional form reasonably well. Typical semilogarithmic plots for three runs using 304 stainless steel are displayed in Figure 13 along with the baseline quartz run. Single exponential dependence over at least two characteristic times, τ, is observed for the stainless steel data. The zero time mark was arbitrarily taken to be the peak in the absorption curve, I', (see Figure 12).

Curve I in Figure 13 was obtained for NF_2 in contact with virgin stainless steel while curves II and III were obtained after 15 and 30 min passivation periods, respectively. These data indicate that the characteristic times for NF_2 loss increase monatonically with increasing time of exposure to NF_2, suggesting a passivation effect. Similar behavior was observed for the other metals that were investigated. Figure 14 displays the three characteristic NF_2 loss times as a function of NF_2 exposure for

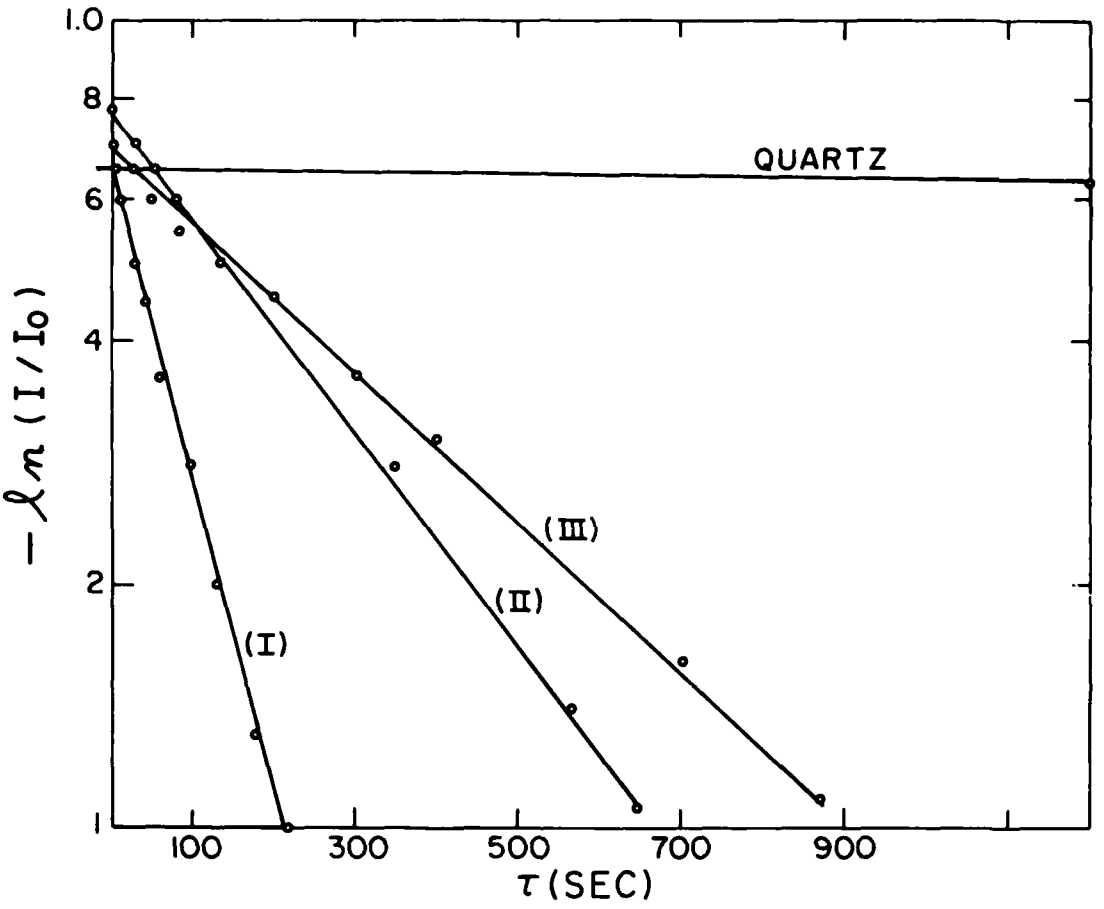

J9525

Figure 13 Semilog Plots of NF_2 Loss Rate in 304 Stainless Steel and Quartz

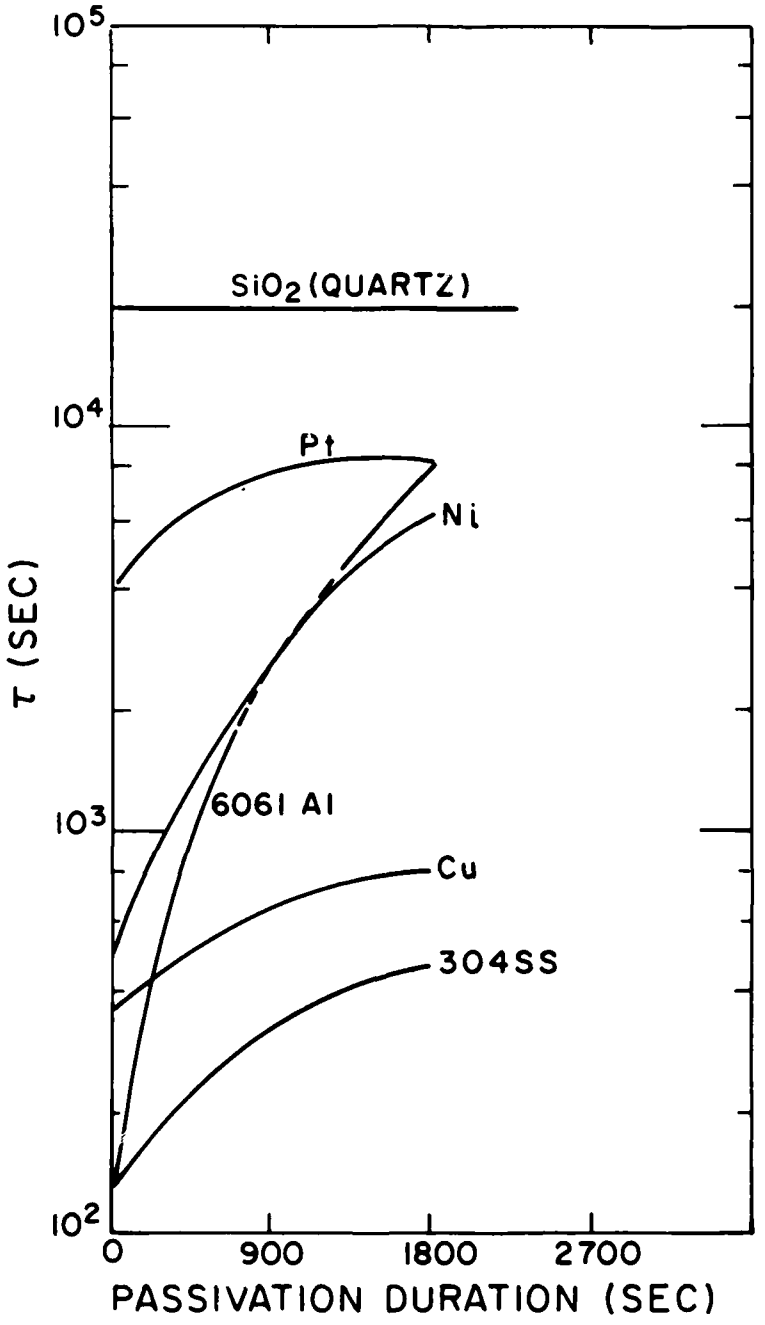

Figure 14 Characteristic Loss Rates for SiO_2, 6061 Aluminum, Nickel, Platinum, 304 Stainless Steel and Copper as a Function of NF_2 Exposure Time

304 stainless steel, copper, nickel, platinum and 6061 aluminum. The reaction rates with aluminum, platinum and nickel are slower than the copper and stainless steel rates. Also, from the slopes of these curves, it appears that the slower reacting materials show a larger passivation effect (i.e., a larger incremental decrease in characteristic time), while the more rapidly reacting materials like copper and stainless steel show a smaller passivation effect.

The most likely explanation for the loss of NF_2 can be explained by heterogeneous chemical reactions forming a strong metal fluoride bond via

$$NF_2 + M \rightarrow NF + MF \qquad (9)$$

where M indicates the metal surface. The reactions forming metal fluorides are favored thermodynamically over the formation of metal nitrides. At present, it is not possible to develop a quantitative model which can predict the observed rates and also explain the differences in rates for different metals. The slow rates measured for aluminum may be the result of the presence of a protective aluminum oxide layer which may be inert to NF_2. The observed NF_2 loss rate then may reflect the slow diffusion of NF_2 through the oxide layer to the bare metal where reaction can take place. Similar consideration may hold for the other slow reacting materials.

3. NF_3 Loss Rates

As is discussed in Section II, the reactivity of NF_3 on Ti and Ni surfaces was measured as a function of temperature using a mass spectrometer to monitor the decay of NF_3. In order to assess the effect of heterogeneous chemistry of NF_3 in an XeF laser in which the laser mixture is recycled, we have measured the reactivity of NF_3 with various surfaces with which the NF_3 could come into contact. Measurements similar to those shown in

TABLE 2. PHYSICAL PROPERTIES OF REACTANTS AND TYPICAL NF_3 DECAY TIMES AT 200°C

METAL	VOID VOLUME (cc)	PACKING FRACTION %	AVG. RADIUS (cm)	τ AT 200°C (sec)
Ti	396	29	0.35	75
Ni	365	32	0.35	1250
QUARTZ	240	55	0.7 x 2.4	2700
Al	230	60	0.32	4500

Figures 7b and 8b suggest an ordering of the reactivity of these surfaces to NF_3. The reader is referred to Section II.B for a detailed discussion of the apparatus and experiment used to investigate heterogeneous loss of NF_3. The results of these measurements are summarized in Table 2. is the time for the NF_3 signal to e-fold at 200°C. The other columns give some of the parameters of the reactant surfaces used. The reactor is made of stainless steel and has a volume of 550 cm^3. Material samples were used in the form of shot and the fourth column gives the average radius of each individual shot.

The loss rate with titanium is clearly faster than with any of the other materials. This is due to the formation of highly volatile TiF_x compounds, whereas for Ni and Al, refractory fluorides are formed that have negligible vapor pressure at 200°C. The quartz case is interesting because volatile SiF_4 could conceivably evolve as a product. However, the very slow loss rate suggests that the fluorine ligands of NF_3 do not readily displace the oxygen in SiO_2. This is in contrast with the well known rapid etching of quartz by HF (or F_2/H_2O mixtures) that also evolves SiF_4. The aluminum results could also be explained by the presence of an oxide layer which inhibits the reaction of fluorine compounds with metals. Similar results were found in the NF_2/aluminum and NF_2/quartz studies reported in Section III.D.2.

The reaction of NF_3 with a metal surface leads to the formation of a metal fluoride and NF_2, via

$$NF_3 + M \rightarrow MF + NF_2 \qquad (10)$$

where M is the metal surface. Directly monitoring the NF_2 formation in reaction (10) at 52 amu is difficult since the major species in the cracking pattern of NF_3 is NF_2 and as shown in

Section III.D.2 when NF_2 is formed it also reacts with the metal surface via

$$NF_2 + M \rightarrow MF + NF. \qquad (9)$$

The NF presumably decays to ultimately form N_2 and fluorine compounds. We have not been able to quantitatively determine all the NF_x decay rates on metal surfaces using the mass spectrometer although we have seen an overall decay of several NF_x species.

IV. ROLE OF NF_2-RADICALS ON XeF LASER PERFORMANCE

In an effort to investigate the impact of NF_2-radicals on laser operating characterstics, we utilized N_2F_4 as a source for these radicals. At the appropriate mole fractions of halogen fuel used in XeF laser mixtures, N_2F_4 is $\sim$1% dissociated at 300°K, 80% dissociated at 400°K and >99% dissociated at 500°K at 1 AMG total pressure. For 2 AMG, these values are $\sim$1%, 67% and >99%, respectively.

Using these values for the degree of dissociation and the reaction stoichiometry, i.e.,

$$N_2F_4 \rightarrow NF_2 + NF_2$$

we were able to systematically investigate the influence of the substitution of NF_2-radicals for NF_3 in laser mixtures. From earlier experiments, we had shown that NF_2 radicals and their parent compound, N_2F_4, could be used as a halogen donor by demonstrating lasing (see Figure 15). These experiments were carried out at high current densities, at 3 AMG density, and detrimental effects such as electron quenching were believed to be dominant and account for the reduction in performance compared to NF_3.

Under this program, experiments were performed using e-beam excited laser mixtures at various current densities, mixture pressures, mole fractions and temperatures. The apparatus used for these measurements has been previously described.[25-28] It

---

(25) Trainor, D.W. and Jacob, j.H., J. Chem. Phys. 72, 3646 (1980).

(26) Rokni, M., Jacob, J.H., Mangano, J.A. and Brochu, R., App. Phys. lett. 30 458 (1977).

(27) Trainor, D.W. and Jacob, J.H., Appl. Phys. Lett. 35, 920 (1979).

(28) Trainor, D.W. and Jacob, J.H., App. Phys. Lett. 37, 675 (1980).

(0.2% HALOGEN DONOR/0.5% Xe/BAL Ne)

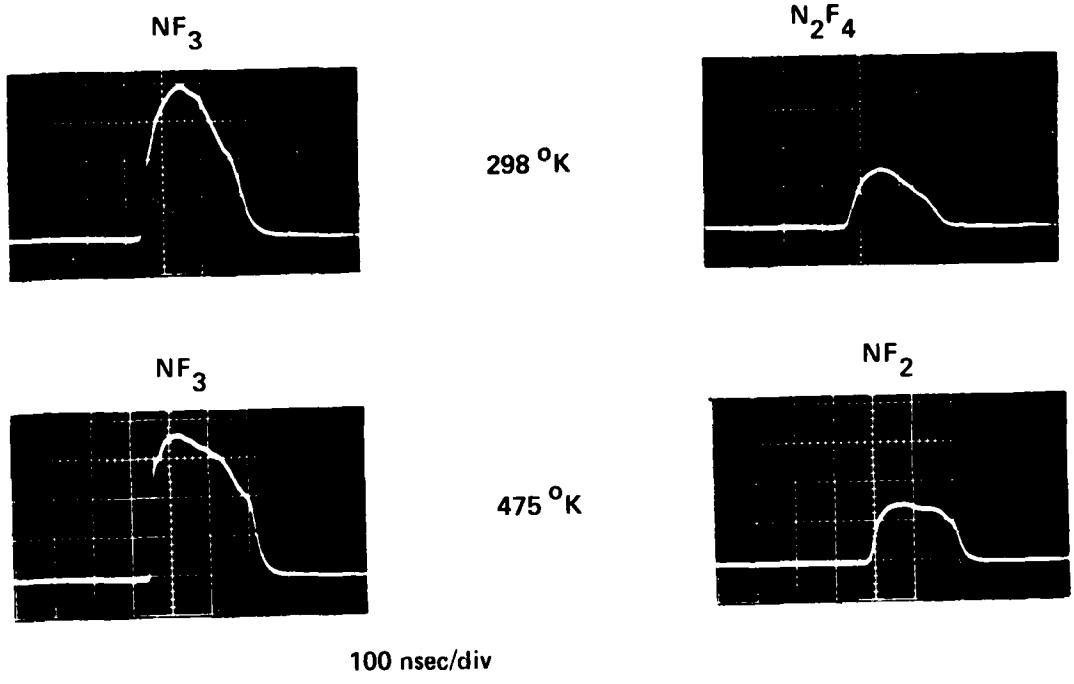

Figure 15 XeF Lasing with NF_3, N_2F_4 and NF_2 Donors

consists of a spatially uniform, high energy e-beam originating from a broad area cold cathode constructed of a series of tantalum blades. The electrons are constrained by an applied external magnetic field and enter the reaction cell through a 2-mil aluminized kapton foil. The gas mixtures in the reaction cell are irradiated by the 250 keV, 10A/cm^2 or 18 A/cm^2 e-beam having a pulse-length of 300 nsec. The mixtures studied were 0.2% fluoride compound (NF_3, NF_2 or N_2F_4 and mixtures thereof), 0.5% xenon and the balance neon at total densities from 1 to 3 AMG. The laser cavity was constructed of stainless steel with flat quartz windows fastened to the cell with holders utilizing Viton o-rings as vacuum seals. The entire cell was capable of being heated to over 500^{o}K.

Mixtures were made in 5 liter stainless steel cylinders utilizing neon (Cryogenic, 99.999%), xenon (Cryogenic, 99.9995%), NF_3 (Air Products) and N_2F_4 (Air Products). The mixture to be studied was introduced into the hot cell and the e-beam fired at times chosen to explore gas-solid chemistry effects as well as laser kinetic issues. For example, after filling the reaction vessel with a standard laser mix of 0.2% NF_3, 0.5% Xe and 99.3% Ne, the e-beam could be fired after $\sim$30 sec. This allowed sufficient time for the mix to come to thermal equilibrium with the cell wall temperature and permit the operator to charge and fire the e-beam. In this way, laser data as well as sidelight fluorescence data were collected. Alternately, the gas could be fired on repeatedly and information on its effective residence time be obtained. Since the cell was primarily constructed of stainless steel, some correlation with the data described in Section III could be expected. By repeating this procedure with different mole fractions of NF_3/NF_2 at constant Xe and neon, information concerning the role of NF_2 radicals could be obtained.

With regard to the issue of residence time, consider the data in Figures 16 through 18. These data were collected at 2 AMG density, 500^{o}K by monitoring XeF* population via the radiation

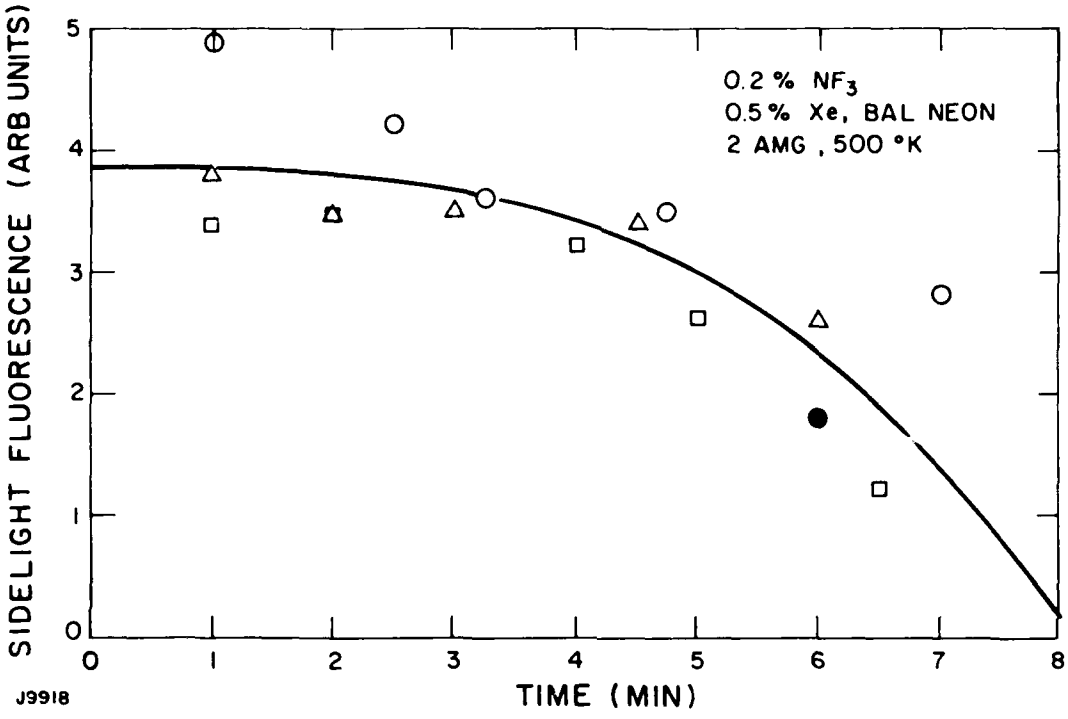

Figure 16 XeF* Sidelight Fluorescence as a Function of Residence Time for Repeated Irradiation of a Gas Mixture of 0.2% NF_3, 0.5% Xe, and 99.3% Ne. (O,Δ,□,● represent experiments conducted on the same nominal mixture at different times.)

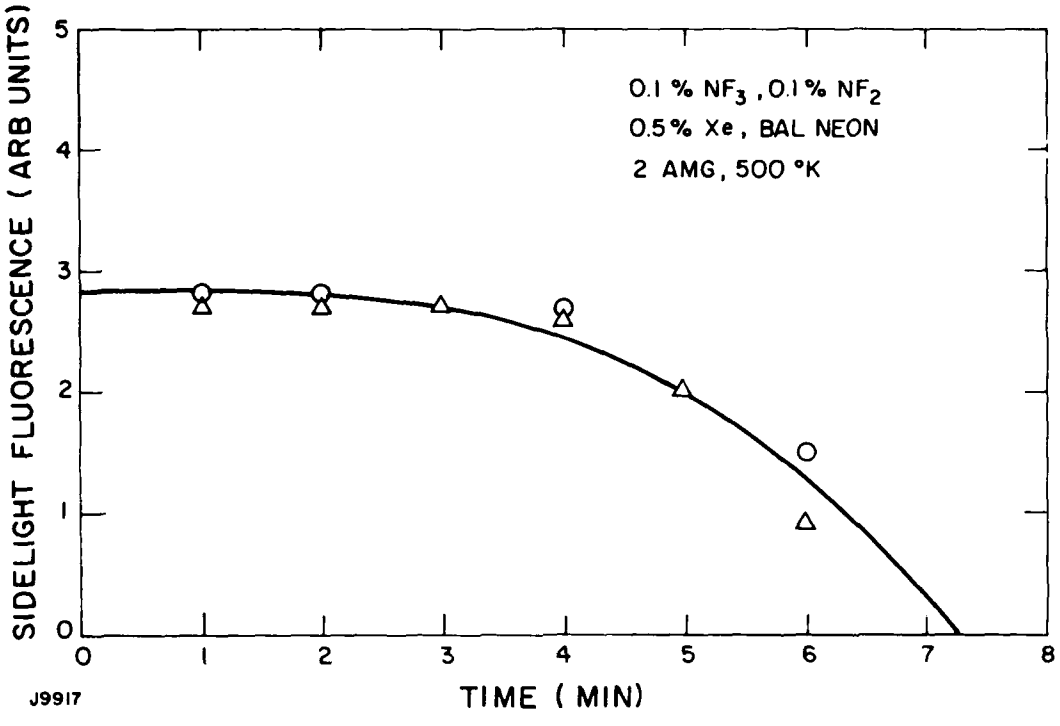

Figure 17 XeF* Sidelight Fluorescence as a Function of Residence Time for Repeated Irradiation of a Gas Mixture of 0.1% NF_3, 0.1% NF_2, 0.5% Xe, 99.3% Ne. (O, Δ represent experiments conducted on the same nominal mixture at different times.)

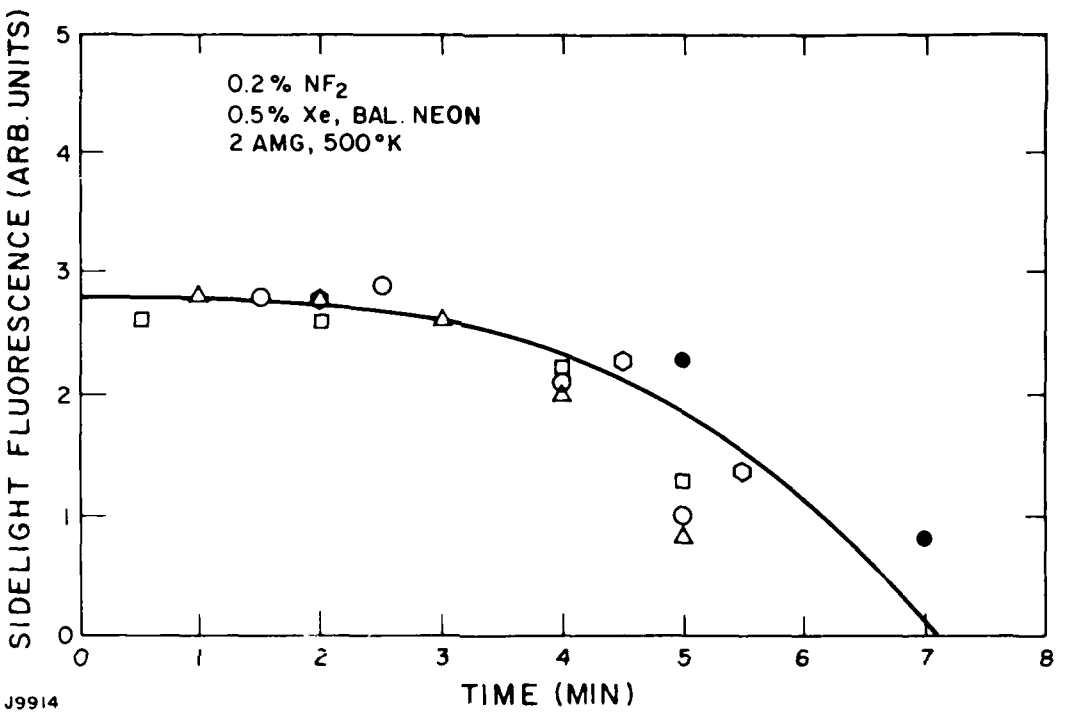

Figure 18 XeF* Sidelight Fluorescence as a Function of Residence Time for Repeated Irradiation of a Gas Mixture of 0.2% NF_2, 0.5% Xe and 99.3% Ne. (O, Δ, □, ⬡, ● represent experiments conducted on the same nominal mixture at different times.)

detected through a sideport using a filtered photodiode. Individual symbols represent repeated irradiation on the same mix at the times indicated. Between fills, the cavity was evacuated prior to repeating the series. The solid datum on Figure 16 at 6 min indicates that within the data scatter, the decrease of the observed fluorescence with time is independent of the e-beam irradiation, i.e., it most likely is due to heterogeneous chemistry effects as were discussed in Section III.

Similar comments are appropriate for the 0.2% NF_2 and 50/50 mixtures in Figures 17 and 18. Attempts to passivate this cell to extend the residence time were not effective (see Figure 19). From these data, we conclude that for residence times shorter than 2-3 min, the data are representative of a fresh fill and should be relatively comparable with regard to NF_2 vs NF_3 effects, etc. It is also in qualitative agreement with the observations reported in Sections II and III that NF_2 and NF_3 react rather rapidly with stainless steel at elevated temperature.

Using the technique, therefore, of filling the laser cavity and operating the excitation pulse at short times after the fill, information concerning the effect of replacing NF_3 with NF_2 on the sidelight fluorescence as well as laser output could be collected. The behavior of laser sidelight is an indication of the coupled effects of formation and quenching processes,[29-32] whereas the laser output includes additional effects such as absorption.

---

(29) Rokni, M., Jacob, J.H., Mangano, J.A. and Brochu, R., App. Phys. Lett 31, 79 (1977).

(30) Rokni, M., Jacob, J.H. and Mangano, J.A., Phys. Rev. A 16, 2216 (1977).

(31) Jacob, J.H., Rokni, M., Mangano, J.A. and Brochu, R., App. Phys. Lett. 32, 109 (1978).

(32) Rokni, M., Jacob, J.H., Mangano, J.A. and Brochu, R., App. Phys. Lett. 32, 223 (1978).

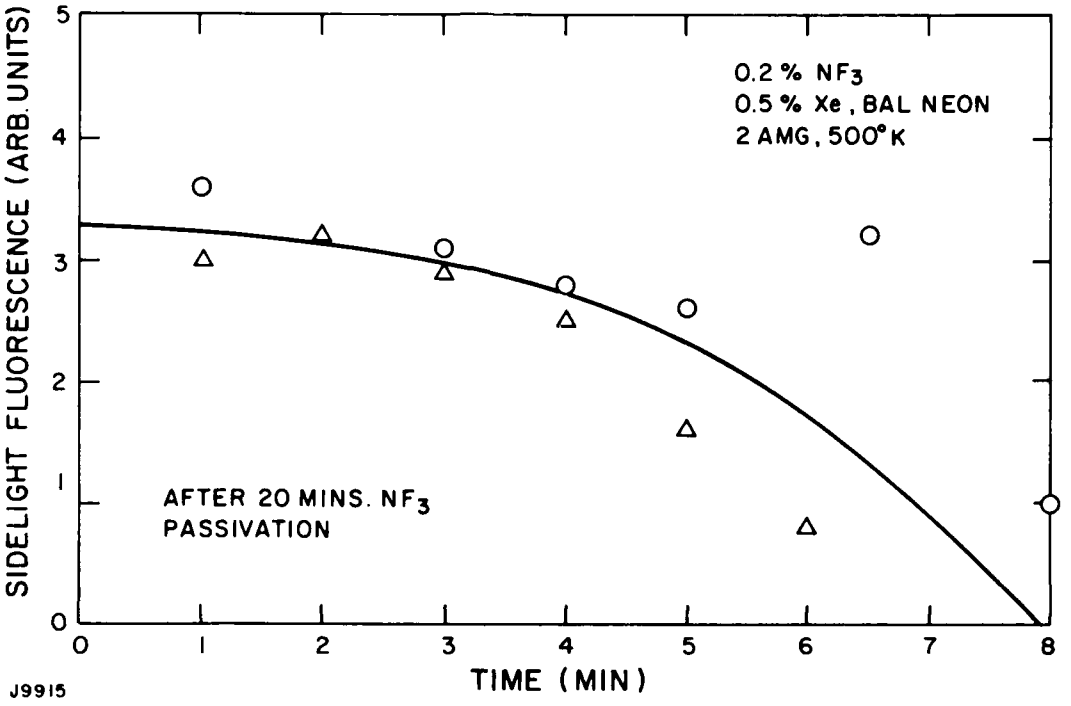

Figure 19 XeF* Sidelight Fluorescence as a Function of Residence Time for Repeated Irradiation of a Gas Mixture of 0.2% NF_3, 0.5% Xe and 99.3% Ne After Pasivation for 20 Minutes. (O, Δ represents experiments conducted on the same nominal mixtures at different times.)

From sidelight and laser pulse temporal signals plots of the maximum peak height vs time (or mix) were obtained. In Figure 20 is shown the effect of increasing the fraction of NF_2 relative to NF_3 at constant overall fractions of 0.2% halogen. These sidelight data indicate NF_2 is a reasonable source for formation of XeF* and/or its quenching influence is similar to NF_3; however, there is some loss in overall signal. One possible model might be that the formation reactions which produce the upper laser states are similar with NF_2 as a donor with similar branching ratios, but the quenching reactions may be more significant when NF_2 is the halide donor. This could be due to an increase in electron density expected when operating with NF_2, since its dissociative electron attachment rate constant is smaller.[33] Since electron quenching may contribute as much as 30% for these experimental conditions,[25] if the electron number density increases a factor of 2 for a 100% NF_2 laser mixture, one would expect the signal to decrease by $\sim$ 25% which is similar to what is observed. This, of course, is speculative; to fully unravel the kinetic details of the impact of NF_2 radicals, an entire kinetic program would be needed.

Similarly, the peak height of the laser pulse has been plotted in Figure 21. These data show significant degradation in the laser output when mixtures containing as little as 25% NF_2 are lased. Subsequent experiment using NF_3 showed no degradation. Since these data were obtained at 500^{o}K in this stainless steel laser cavity, one explanation would involve the presence of an absorber at the laser operating wavelength. Since NF_2 has an absorption maximum at shorter wavelengths,[24] either sequential dissociation to produce NF must be invoked and/or the absorber may arise as a result of heterogenous reactions. Regardless, the

---

(33) Trainor, D.W. and Jacob, J.H., (Unpublished).

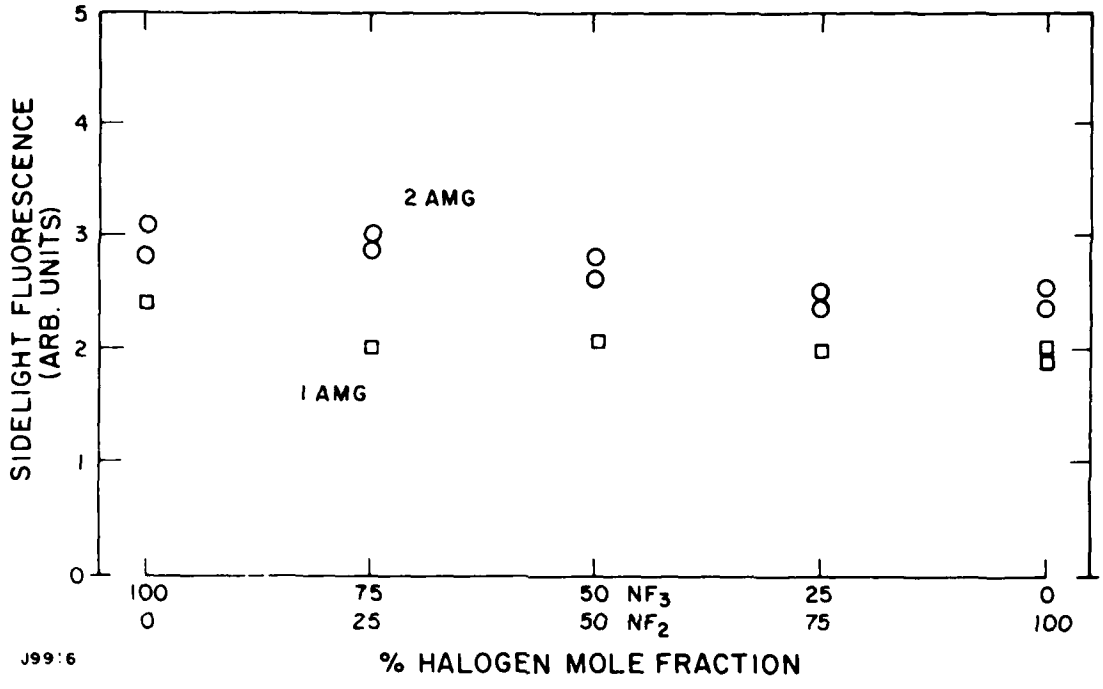

Figure 20 XeF* Sidelight Fluorescence for Various Mole Fractions of NF_2/NF_3

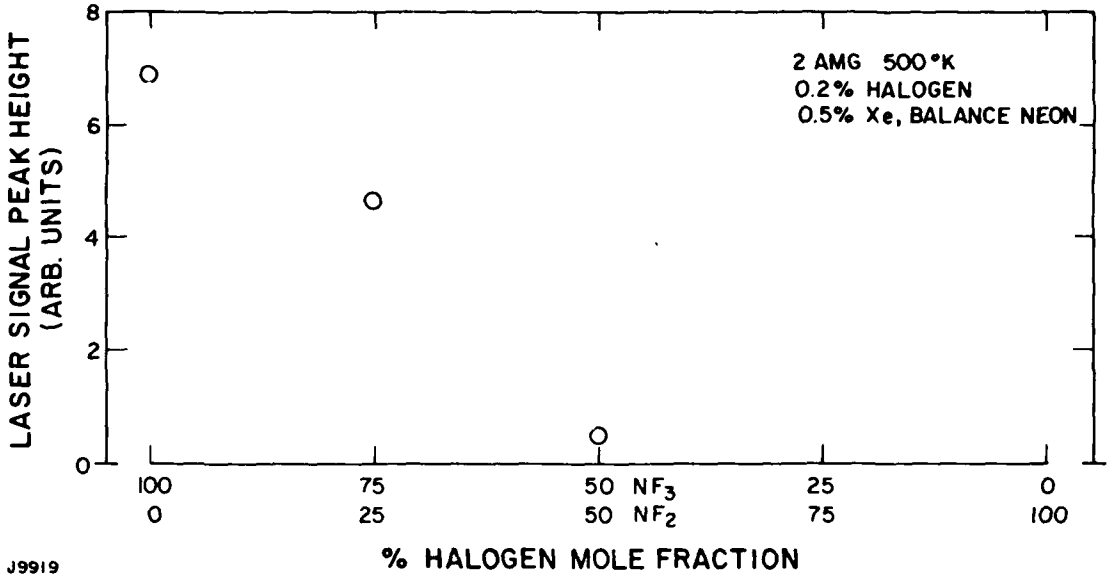

Figure 21 XeF* Laser Peak Height for Various Mole Fractions of NF_2/NF_3

laser degrades significantly. This, of course, is not in accord with the laser signals shown in Figure 15. These earlier data suggested that NF_2 is an effective donor, whereas in this cell, at this current density, NF_2 does not appear to be an effective halogen fuel. Significantly, these earlier data were taken in a cell of different construction and suggest that the cell composition has a significant impact on the laser results. This is in qualitative agreement with the results described in Section III where various metals were found to be more or less reactive than stainless steel. Clearly, more information regarding the influence of the cells construction on laser operation needs to be collected before projections to closed-cycle operation can be carried out.

*U.S.Government Printing Office: 1981 — 559-003/2005

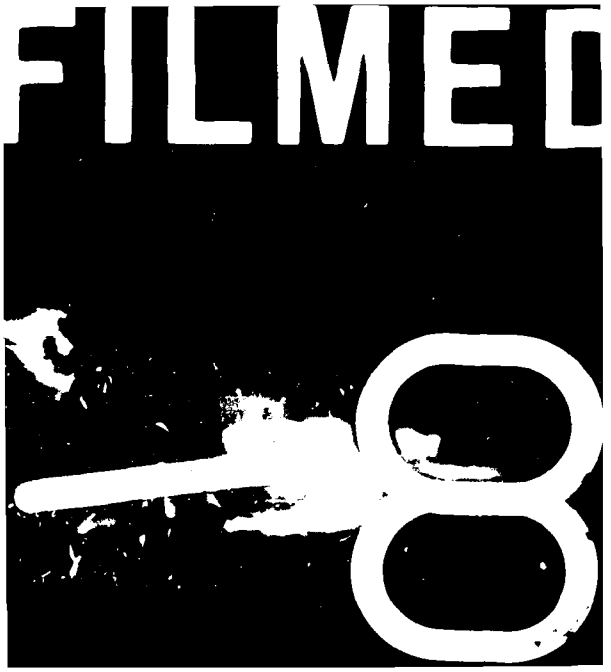
FILMED